Synthesis and Characterization of Molybdenum N-Heterocyclic Phosphenium and Phosphido Complexes

Undergraduate Research Thesis

Presented in partial fulfillment of the requirements for graduation *with honors research distinction* in Chemistry in the undergraduate colleges of The Ohio State University

by

Riley Kelch

The Ohio State University

April 2021

Project Advisor: Professor Christine M. Thomas, Department of Chemistry and Biochemistry

Acknowledgements

I would like to express my sincerest gratitude to my advisor Professor Christine Thomas. Her guidance has been crucial to the advancement of this project and to my development as a scientist, thinker, and all-around person. Additionally, I must thank my long-time graduate student mentor, Andy Poitras. He taught me how to function in a glovebox, guided me through science before I knew anything about (in)organic chemistry, and took an egregious number of NMRs for me, amongst other things. I also want to thank Greg Hatzis and Leah Oliemuller for being great mates on the NHP project in Michael Scott as well as TJ Yokley and Josh Shoopman for thoughtful discussions and for working night shifts with me through the Covid-19 pandemic. I'll end with a list of everyone I've worked with in the Thomas lab, as I'm grateful to all of you.

Prof. Christine Thomas

Dr. Jeffrey Beattie	Josh Shoopman
Dr. Elizabeth Lane	Subha Himel
Dr. Kyounghoon Lee	Nathan McCutcheon
Dr. TJ Yokley	Jeremiah Stevens
Dr. Katie Gramigna	Sean Morrison
Dr. Hongtu Zhang	David Ullery
Dr. Andrew Poitras	Shannon Cooney
Greg Hatzis	Nathan Pimental
Leah Oliemuller	Canning Wang
Nate Hunter	Prof. Ewan Hamilton
Brett Barden	Dr. Curtis Moore

Abstract

In this work, a variety of synthetic and computational studies unified by the theme of cooperativity in catalyst design are described. Although noble metals are used abundantly in the field of catalysis, they are not abundant in the Earth's crust. As such, the strategies of both metal-ligand cooperativity and metal-metal cooperativity offer sustainable alternatives by enabling desirable chemistry at base metals. In both cooperative strategies, the redox burden at a metal is alleviated by a ligand or additional metal that is capable of either chemical modification or direct substrate bond activation. In this work, coordination of a N-heterocyclic phosphine (NHP) pincer ligand to a molybdenum carbonyl fragment is explored. Evidence for both formally phosphenium (NHP^{+}) and phosphido (NHP^{-}) molybdenum carbonyl complexes synthesized from it are presented, highlighting the ligand's redox non-innocence. The phosphenium complex or a derivative thereof may be capable of σ bond activation, though reactivity is not explored in this work.

Table of Contents

Introduction

N-heterocyclic carbene (NHC) ligands have become ubiquitous in coordination chemistry since their initial isolation in 1991.[1] When complexed to metals, their strong σ-donor and weak π-acceptor properties have proven useful for a wide range of homogeneous catalytic transformations including cross-couplings, hydrogenations, cycloadditions, and asymmetric reactions.[2–12] Although isoelectronic to NHCs, N-heterocyclic phosphenium ligands have received comparatively little attention in the literature. This could be due to their wildly different electronic properties: while NHCs are strong σ-donors and weak π-acceptors, NHPs are weak σ-donors and strong π-acceptors.[13] Nevertheless, interest in NHP chemistry has grown in recent years and has even sparked interest in congeners containing nitreniums[14–22] and heavier pnictogens.[22–24] Furthermore, the open coordination site of an NHP potentially allows for metal-ligand cooperative reactivity rather than traditional metal-centered-only reactivity. This is facilitated by the NHP's ability to convert between a neutral phosphine and either a positively charged phosphenium or negatively charged phosphido ligand, alleviating the redox burden often borne solely by the metal. This type of reactivity could lead to the discovery of new catalytic cycles that do not require precious metals.

Earliest Phosphenium Cations

Before the synthesis of the first NHP^+, linear, two-coordinate phosphorus was first reported in 1964 by Hoffmann in a class of compounds known as phosphacyanines (Figure 1).[25] In these species, the cationic charge is stabilized by extensive delocalization across heterocycles. Subsequently, partial multiple-bond character is associated with the phosphorus atom. Stabilizing

motifs such as these are generally required to isolate phosphenium cations because two-coordinate cationic phosphorus is well-poised for attack by nucleophiles.

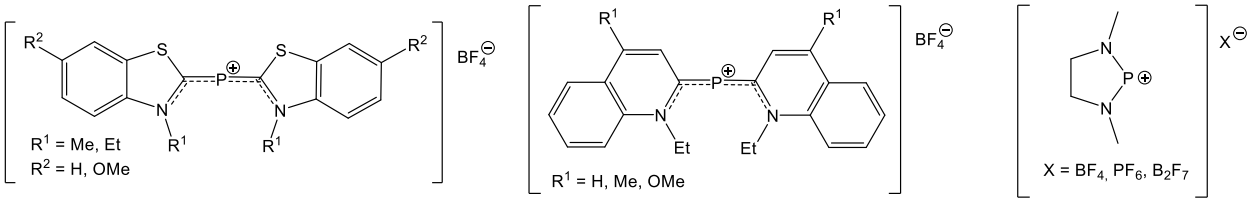

Figure 1. Hoffmann's two phosphacyanines (left) and Fleming's NHP^+ (right)

The first isolated NHP cation was reported in 1972 by Fleming nearly 20 years before the first report of Arduengo's free NHC (Figure 1).[26] In addition to being a structurally novel compound, this [NHP][PF_6] had a highly unusual ^{31}P NMR chemical shift of 274 ppm, corroborating the structural assignment by indicating an extremely deshielded phosphorus atom.[26] For reference, the farthest downfield chemical shift for lists of "typical" phosphorus compounds is 245 ppm for PF_2Me.[27] Fleming's NHP^+ species was generated by halide abstraction from a halophosphine precursor, a method that has remained useful in more recent literature.[28–30] The NHP^+ is distinct from Hoffmann's phosphacyanines in that the majority of the positive charge is localized on phosphorus. In lieu of adjacent resonance-stabilizing aromatic heterocycles, Fleming's NHP^+ is stabilized by π donation to P from neighboring N atoms.

Non-Innocent Ligands

Non-innocent ligands are involved in two primary types of reactivity: (1) participation in a catalytic cycle by accepting/donating electrons or (2) actively forming/cleaving covalent bonds with the substrate.[31] Such ligands are key to the strategy of metal-ligand cooperativity, which is

unique from oxidative addition in that the oxidation state of the metal remains unchanged (Figure 2).[32,33] Recent examples include base metal systems for hydrogen transfer chemistry that involve conversion between amide/amine ligand functionalities[34–36] or disrupting aromaticity of ligand frameworks.[37,38] Examples of ligands displaying redox non-innocence include pincer [ONO] and [SNS] complexes reported by Heyduk that are stable as mono-, di-, and trianions.[39,40]

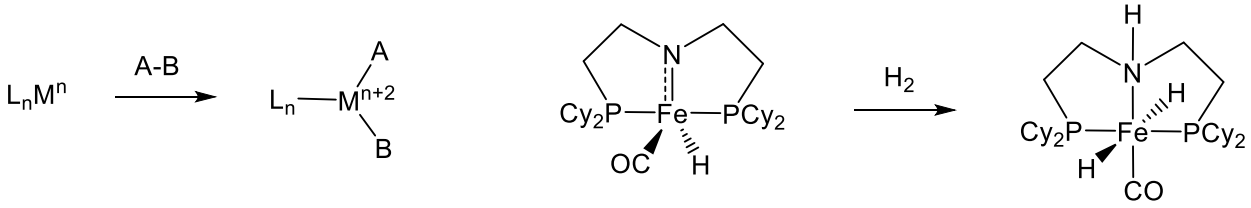

Figure 2. Oxidative addition (left) vs. a metal-ligand cooperative amide/amine system[34] (right)

Although NMR is a powerful spectroscopic tool for characterizing ligands that form bonds to the substrate such as in the amine/amide bifunctionality above, systems with redox non-innocent ligands that do not directly activate bonds may require alternative characterization methods. For example, nitrosyl, the prototypical redox non-innocent ligand, is commonly found in either the NO^+ or NO^- oxidation state (Figure 3). In its cationic form, it adopts a linear geometry, but in its two-electron reduced form, it adopts a bent geometry.[41] This structural change is observable in the solid state by single-crystal X-ray diffraction, often allowing for facile oxidation state assignment. In addition, the N-O bond order varies with the charge of the NO ligand, allowing for additional characterization by IR spectroscopy.

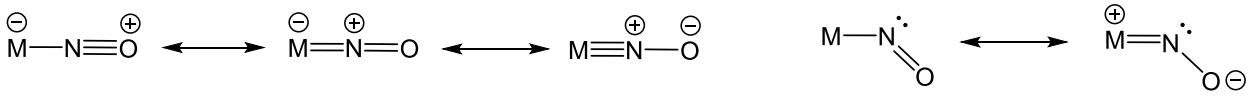

Figure 3. NO binding modes and resonance structures. NO^+ (left) vs. NO^- (right)

Although a wide array of physical methods can be used to characterize metal complexes bearing NO or analogous ligands (e.g. NHPs), it may remain difficult to assign proper electronic descriptions to such complexes. This issue has been long-observed in the field of coordination chemistry and is discussed in a 1974 review by Enemark and Feltham.[42] Enemark and Feltham note complexes for which there is ambiguity between M^n/NO^+, M^{n+2}/NO^-, or perhaps even $M^{n+1}/NO\cdot$ descriptions and instead proffer a more all-encompassing notation: $\{MNO\}^m$.[42] This notation has remained useful through the present day. One recent example is work by Zhang on four-coordinate copper halonitrosyl $\{CuNO\}^{10}$ complexes capable of reversible NO· evolution and binding.[43] In this report, complexes featuring square planar Cu with bent nitrosyl ligands are observed, perhaps suggesting a Cu^{3+}/NO^- or $Cu^{2+}/NO\cdot$ electronic structure. However, the compound's EPR silence suggests a Cu^{3+}/NO^- or Cu^+/NO^+ description. Detailed CASSCF calculations provide the best evidence for a $Cu^{2+}/NO\cdot$ description, which is consistent with observed reversible NO· evolution and binding.[43]

An additional notable example of ambiguity from structural data is a mid-2000s heated debate over borane ligands in transition metal complexes. In the view of Parkin, Z-type borane ligands should be viewed as formal two-electron oxidants, yielding a description of M^{n+2}/BX_3^{2-}.[44] He reasons that this description better reflects the d^n configuration of the complex and is supported by computational evidence.[45,46] In contrast, Hill posits that M-B bonding can be ambiguous and supports a more all-encompassing notation akin to that of Enemark and Feltham.[47] His description permits a more diverse array of M-B bonding descriptions and is supported by both computational studies and nontraditional boron geometries.[48–50] It is possible that debate over oxidation states in ambiguous systems may be settled by utilizing X-ray absorption near-edge structure (XANES), a type of spectroscopy that excites core-level electrons

and provides quantitative information related to oxidation state. However, it can be difficult to get beamtime for this spectroscopic method. At the end of the day, oxidation states are merely a formalism used for electron bookkeeping; examining a complex's reactivity is often more important than quibbling over notation.[51]

Bonding in NHP Complexes

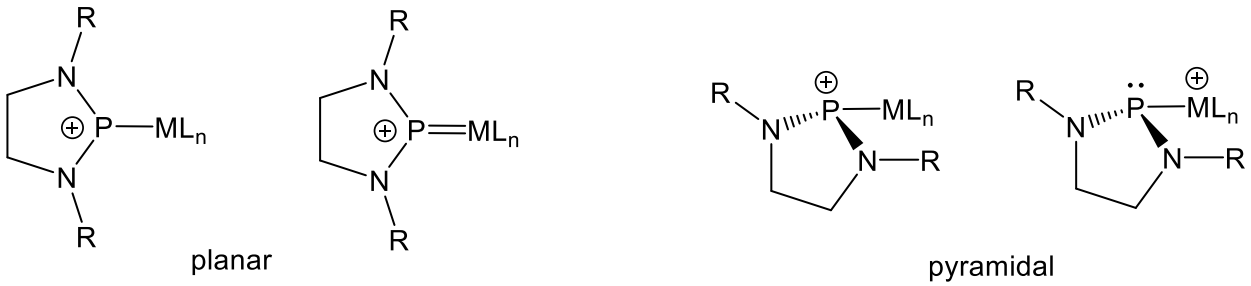

Figure 4. Binding modes of NHP^+/NHP^- ligands

As weak σ donors and strong π acceptors, NHP ligands' electronic properties facilitate multiple possible binding modes when complexed to a metal.[13] These binding modes can be divided into two groups based on the coordination geometry at phosphorus: planar or pyramidal. For planar NHPs, a phosphenium description is necessitated, as the sp^2 hybridization and empty p orbital on phosphorus are required to achieve this geometry. In one planar NHP bonding scenario, the metal-ligand bond is composed solely of a σ donation from the phosphorus lone pair to the metal. In an alternate planar scenario, a sufficiently electron-rich metal can additionally π backbond to the NHP ligand, potentially resulting in a formal metal-ligand double bond. This doubly-bonded planar NHP geometry is commonly observed in the literature, especially in the laboratory of Gudat, which has reported such NHP binding for carbonyl complexes of Cr,[52,53] Mn,[54,55] Fe,[53,56] and Co.[55]

In the alternative geometric scenario, NHPs can adopt a pyramidal geometry about phosphorus. In these cases, assignment of oxidation states can become more difficult. In one binding mode, the NHP cation acts as a Z-type ligand by receiving electron density from the metal in the form of a σ bond. Alternatively, the NHP's oxidizing power may be significant enough to result in a formal two-electron oxidation of the metal, yielding an electronic description of NHP^{-}/M^{n+2}. This binding mode has been observed predominantly by the Thomas lab, including NHP^{-} complexes of Co,[57,58] Rh,[59] Pd,[60,61] and Pt.[60,61] Observation of the NHP^{-} form and divergent geometries has permitted the analogy of NHPs to nitrosyls as redox non-innocent ligands with multiple possible oxidation states. As a final note, NHP ligands are capable of bridging metal centers, typically forming dimeric or trimeric species. This has been observed for both NHP^{+} and NHP^{-} ligands, as well as cases where oxidation states are ambiguous.[54,59,61–65]

Synthesis of NHP Metal Complexes

Multiple routes exist to the formation of NHP complexes. Three are summarized well by Nakazawa in a 2000 review: (1) electrophilic attack of a phosphenium cation to a metal carbonyl or phosphine complex, (2) halide abstraction after a halophosphine is coordinated to a metal, or (3) hydride abstraction after a phosphine is coordinated to a metal (Scheme 1, 2).[66] Method 1 was pioneered by Parry in 1978 by treating $Fe(CO)_5$ with $[NHP][PF_6]$ to generate $[(NHP)Fe(CO)_4][PF_6]$.[67] In the same issue of *JACS*, Paine pioneered Method 2 by reacting a fluorophosphine with $Na[MoCp(CO)_3]$ (Cp = cyclopentadienyl anion). In the reaction, NaF salt is eliminated and a phosphenium cation is generated in situ, yielding $(NHP)MoCp(CO)_3$.[68] Method 1 is by far the most common in the literature for the generation of NHP^{+} complexes.[29,55,56,69–74] Method 3 is largely similar to Method 2, though hydrides are often

removed with Lewis acidic boron reagents[66,75,76] or instead migrate from the NHP to the metal center.[52] An additional route, Method 4, involving both halide abstraction and reduction of a metal complex, has proven useful in the Thomas lab for the generation of both NHP^+ and NHP^- complexes (Scheme 2).[58,74]

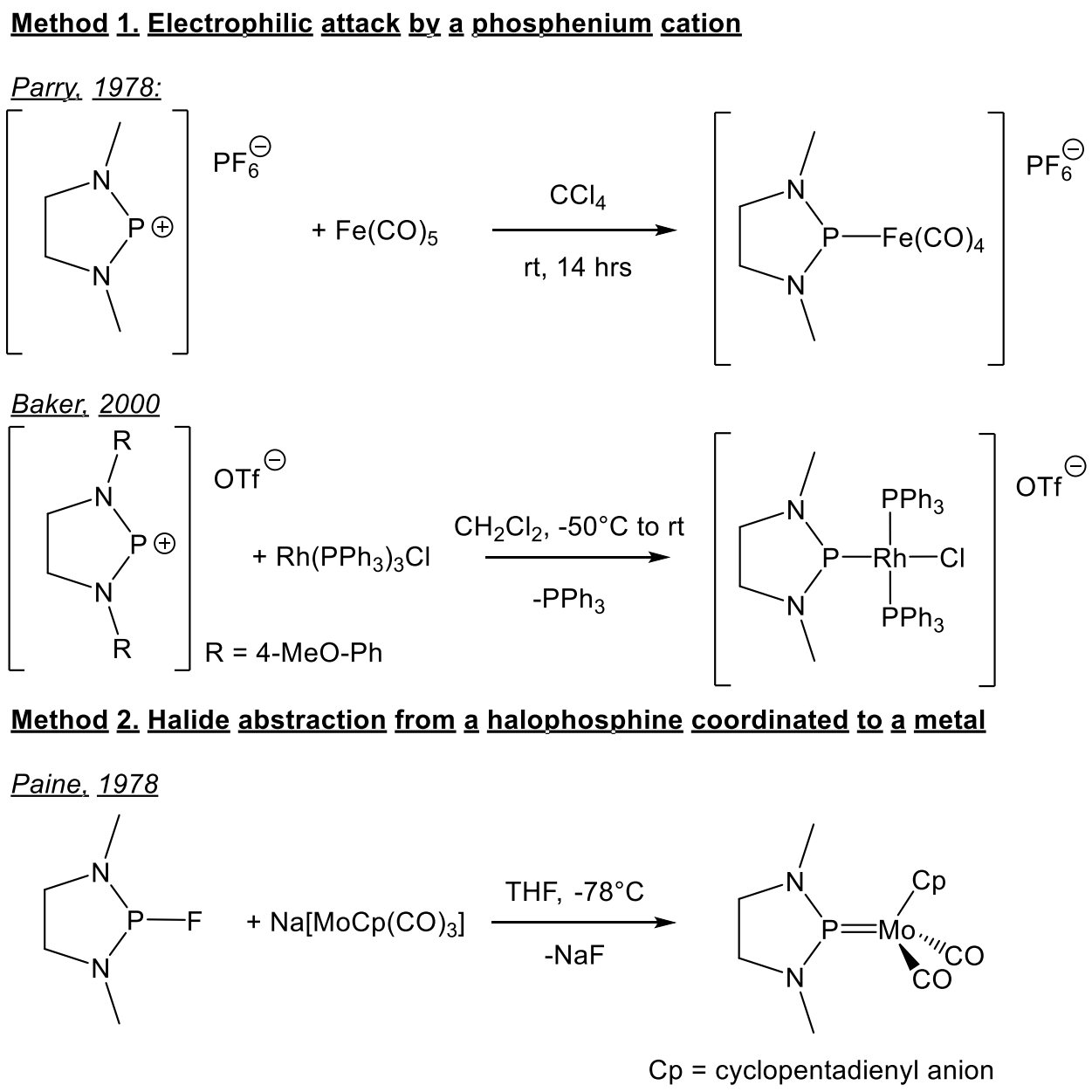

Scheme 1. Synthesis of NHP^+ metal complexes using Methods 1 and 2

Method 3. Hydride abstraction from a phosphine coordinated to a metal

Parry, 1987

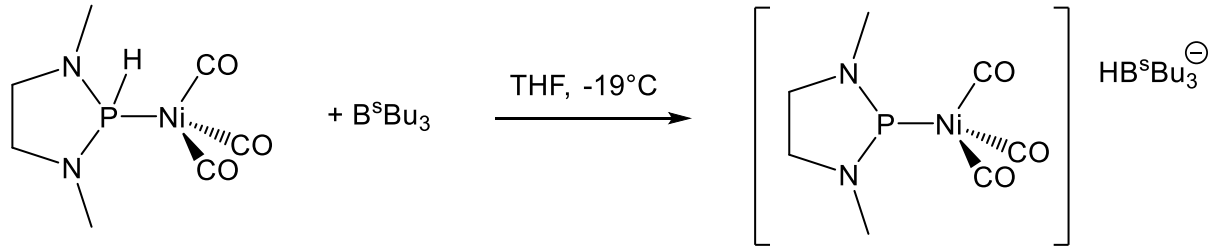

Gudat, 2020

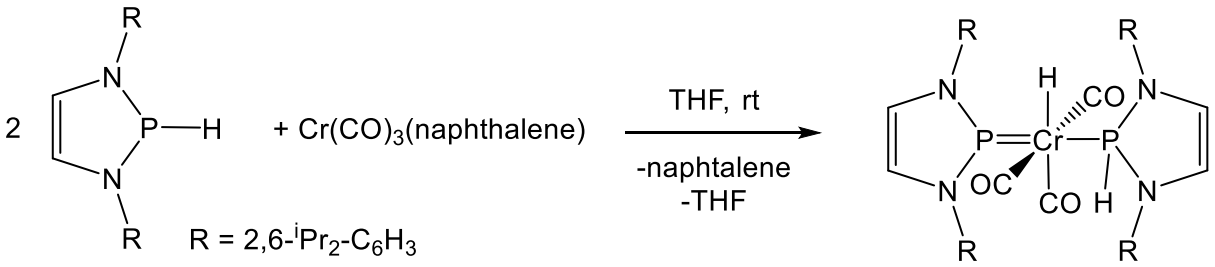

Method 4. Halide abstraction and reduction of a halophosphine metal complex

Thomas, 2017

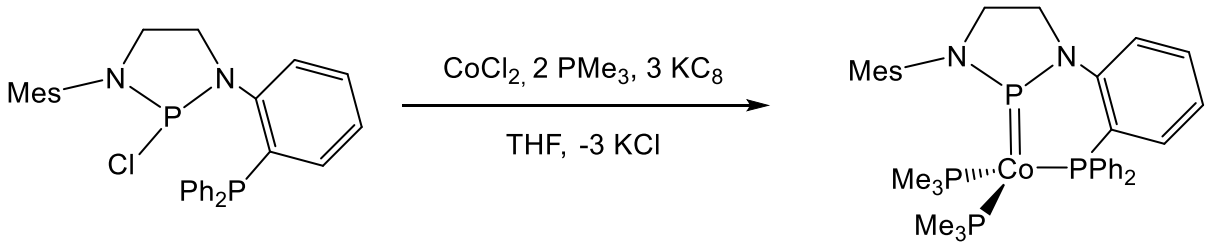

Thomas, 2018

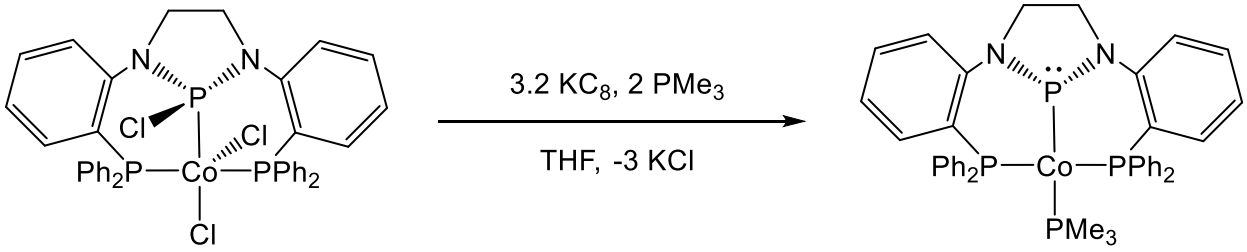

Scheme 2. Synthesis of NHP$^+$/NHP$^-$ metal complexes using Methods 3 and 4

Reactivity of Free NHPs

Before exploring metal-cooperative reactivity of metal complexes bearing NHP ligands, it is important to understand the reactivity of NHPs in the absence of metals. Reactive NHP chemistry is dominated by use of the phosphenium as a Lewis acid stabilized by donation from the adjacent N atoms. One notable analogue that does not feature this type of stabilization is the bis(ferrocenyl)phosphenium ion, which instead features significant intramolecular Fe···P contacts that moderate Lewis acidity.[77] Regardless, the electrophilic character of phosphenium ions has proven useful for a wide range of organic transformations, including reversible cycloadditions[78] and the preparation of phosphazanes from NHP-azides.[79]

As a main group element, the nature of phosphorus's bonds to hydrogen has been particularly well studied. Although NHPs have a proclivity to form phosphenium ions through the formal loss of a halide or hydride, chemistry involving loss of a proton or hydrogen atom has also been explored.[80,81] For example, in one report, the nature of the P-H bond in two NHP-H molecules, one with a large aromatic backbone and one with an alkyl backbone, was compared (Scheme 3).[82] The study found that the NHP-H with the aromatic backbone acted as a moderate hydride and hydrogen atom donor and a poor Brønsted acid while the NHP-H with the alkyl backbone acted as a good hydride donor and moderate hydrogen atom donor with no detected Brønsted acidity. These findings are evidence for the importance of tuning the electronics of an NHP to achieve desired reactivity.

Scheme 3. P-H bond character of select NHP-H molecules

NHPs have also emerged as practical catalysts for select reactions without the need for a transition metal. Kinjo was one of the first to use NHP catalysts, demonstrating the ability to catalyze hydrogenation of N=N double bonds with ammonia borane.[83] The same group has gone on to use NHP catalysts for the hydroboration of carbonyls[84] and regio- and chemoselective hydroboration of pyridines.[85] Additional hydroboration catalysis has been explored by Melen[86] and Speed, the latter of which has reported asymmetric imine hydroboration[87] and air/water stable hydroboration precatalysts.[88] Further examples of specialized reduction catalysis include enantioselective imine reduction reported by Speed[89] and enantioselective reduction of conjugates by Cramer.[90] Since all of these transformations are achieved in the absence of a transition metal, similar or improved activity may be feasible with a metal-NHP cooperative system.

Reactivity of NHP-Metal Complexes

As NHP metal complexes are a relatively recent subject of research, reports of reactivity and catalysis are limited primarily to the labs of Gudat and Thomas. Reports from the Gudat lab have focused primarily on hydrogenation and dehydrogenation chemistry using NHP carbonyl complexes. For example, Gudat's (NHP)$Mn(CO)_4$ complex has proven competent for the dehydrogenation of ammonia borane to primarily cyclotriborazane and B-(cyclodiborazanyl)aminoborohydride (Scheme 4, top).[54] Gudat has more recently reported a $(NHP)_2Cr(CO)_3$ complex capable of reversible metal-ligand cooperative H_2 activation under specific heating and irradiation conditions (Scheme 4, bottom) as well as the photocatalytic hydrogenation of styrene.[52]

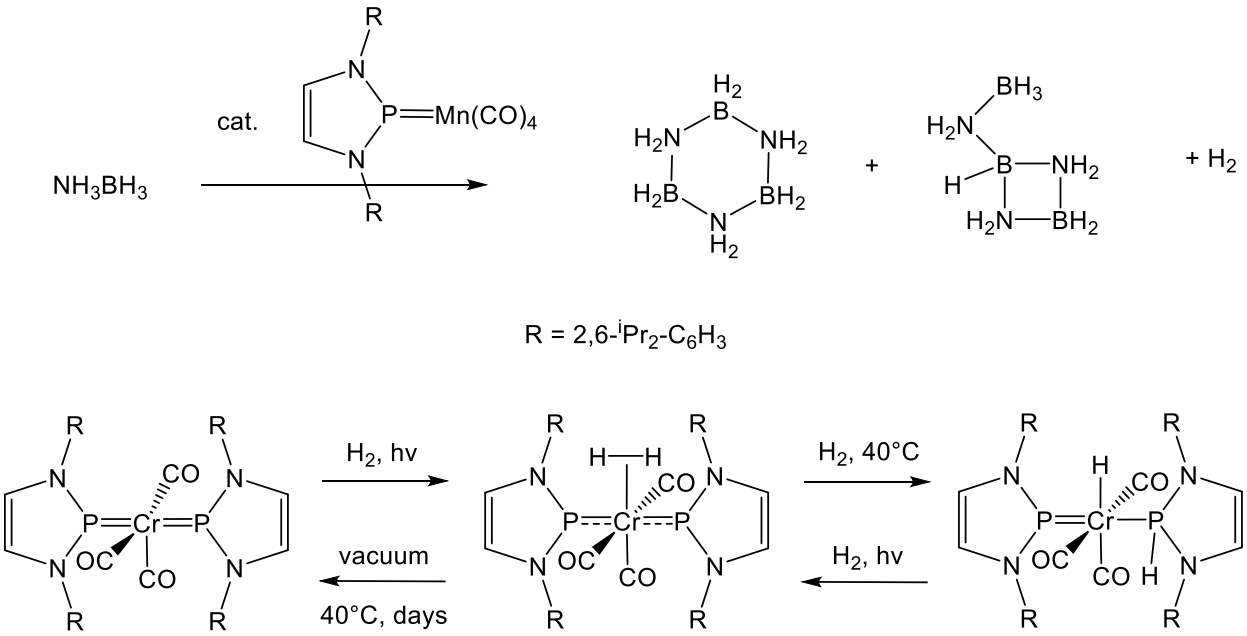

Scheme 4. Gudat's NHP complexes for catalytic (de)hydrogenation

Work in the Thomas lab has focused primarily on phenol/thiophenol activation and dehydrogenation chemistry, especially with late transition metal complexes bearing ancillary phosphine ligands. Such studies have been instructive for understanding the electronic structures of NHPs when incorporated into a pincer ligand framework. For example, Thomas has demonstrated that (PPP)Rh($PMePh_2$) is capable of activating thiophenol, yielding a product with a P-H bond (Scheme 5, top).[59] The observed product is consistent with other evidence that the NHP ligand is formally anionic in this complex. However, reactions with complexes of other late metals reveal the electronic complexity of the (PPP) ligand. Treatment of (PPP)Pt(PPh_3) with thiophenol yields a product analogous to the Rh case, but (PPP)Pt(PPh_3) reacts divergently with alcohols to instead form a product with a P-O bond (Scheme 5, bottom).[60] This type of reactivity with alcohols would be expected for a phosphenium ligand, providing evidence for the NHP's redox non-innocence.

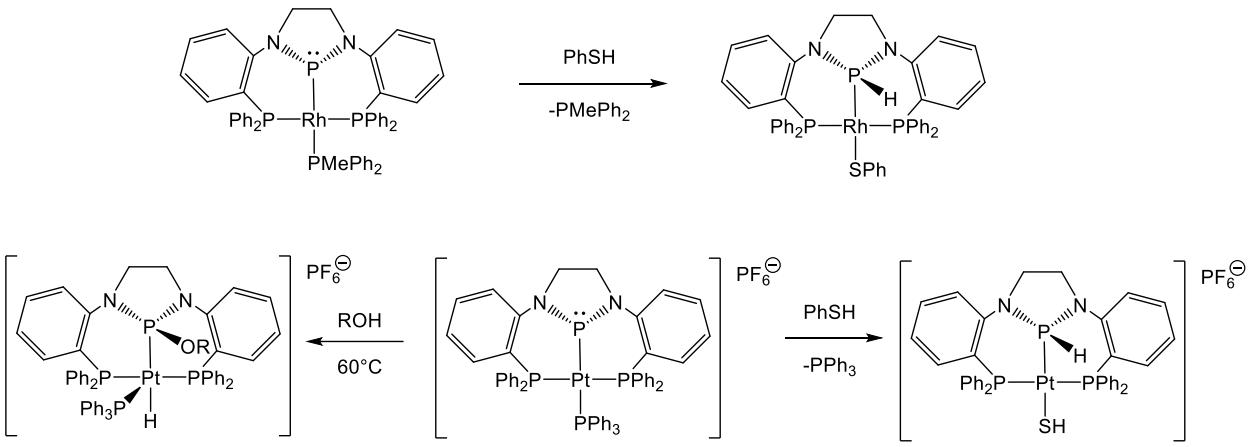

Scheme 5. E-H bond activation by noble metal complexes from the Thomas lab

Exploration of the chemistry of (PPP)Co(PMe_3) in the Thomas lab has led to further curiosity regarding the (PPP) ligand (Scheme 6). Upon treatment with PhOH, the complex reacts to form a product with a P-O bond, analogous to the Pt system.[91] Initial treatment (5 min) of (PPP)Co(PMe_3) with PhSH affords a product featuring a P-H bond, again analogous to the Pt and Rh systems. However, after 20 hours, the initial product surprisingly isomerizes to a more thermodynamically stable product instead featuring a P-H bond. In addition, (PPP)Co(PMe_3) is capable of more challenging reactivity: H_2 activation and ammonia borane dehydrogenation (Scheme 6).[58] Unfortunately, these reactions are stoichiometric rather than catalytic, but they do represent the first reported example of H_2 addition across a first-row metal-phosphorus bond.

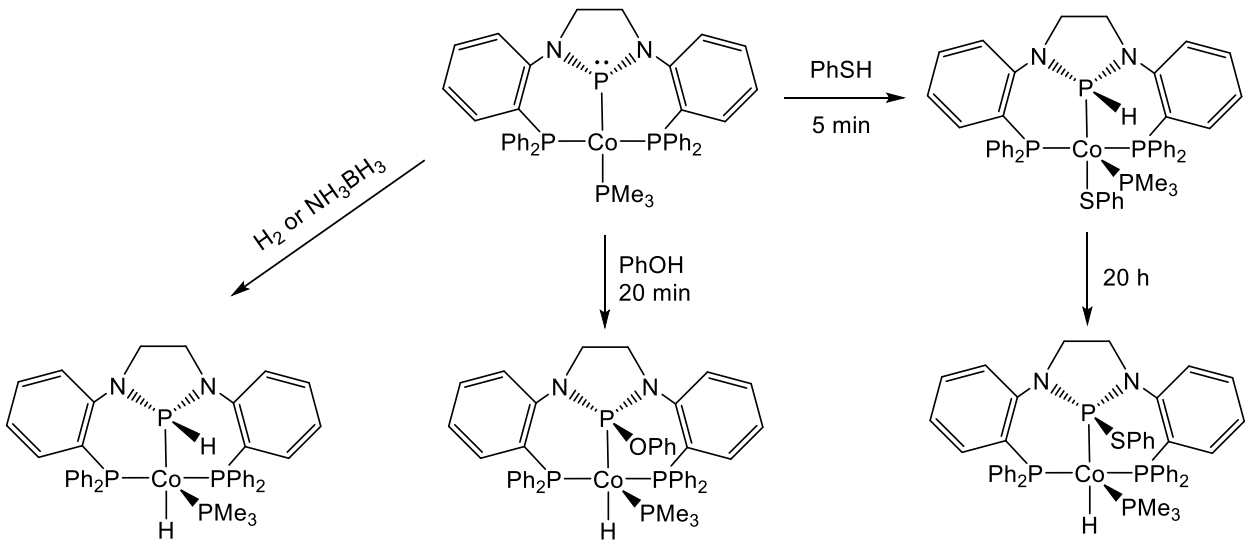

Scheme 6. Reactivity of (PPP)Co(PMe_3)

Synthesis of Molybdenum Pincer Complexes

Pincer ligands have been coordinated to molybdenum numerous times in the literature. Most examples can be grouped into one of two categories: low-valent molybdenum pincer complexes featuring π-acidic ligands or high-valent THF adducts of molybdenum halides. Common metal precursors for the synthesis of such meridional pincer complexes include $Mo(CO)_3(MeCN)_3$,[92–95] $Mo(CO)_2(MeCN)_2(PPh_3)_2$,[96] $Mo(CO)_6$,[97–100] $Mo(CO)_3(THF)_3$,[97] and $Mo(THF)_3X_3$.[101–105] Synthesis of pincer complexes from these precursors generally takes less than a day of stirring in solution; typical reaction conditions include stirring in room temperature THF,[93,96,101] room temperature MeCN,[94] or heating/refluxing in MeCN,[95,98–100] toluene,[92,105] or benzene.[97]

In addition, the commercially available $Mo(CO)_3$(cycloheptatriene) has also been used as a metal precursor. However, the carbonyls of this piano stool complex are arranged in a fac orientation. Although mer pincer complexes have been synthesized from it,[106–108] it may be more useful for the synthesis of fac pincer complexes,[107–112] complexes with tripodal ligands,[113–115]

complexes with bidentate ligands,[107,108] or metal clusters.[116,117] Indeed, it is worth noting that the limited examples of mer pincer complexes synthesized from $Mo(CO)_3$(cycloheptatriene) feature flexible pincer ligands containing ethylene linkers and/or are generated by partial conversion over time from the fac isomer.[107,108]

Results and Discussion

Synthesis of $(PP^{Cl}P)Mo(CO)_3$ as a Phosphenium Precursor

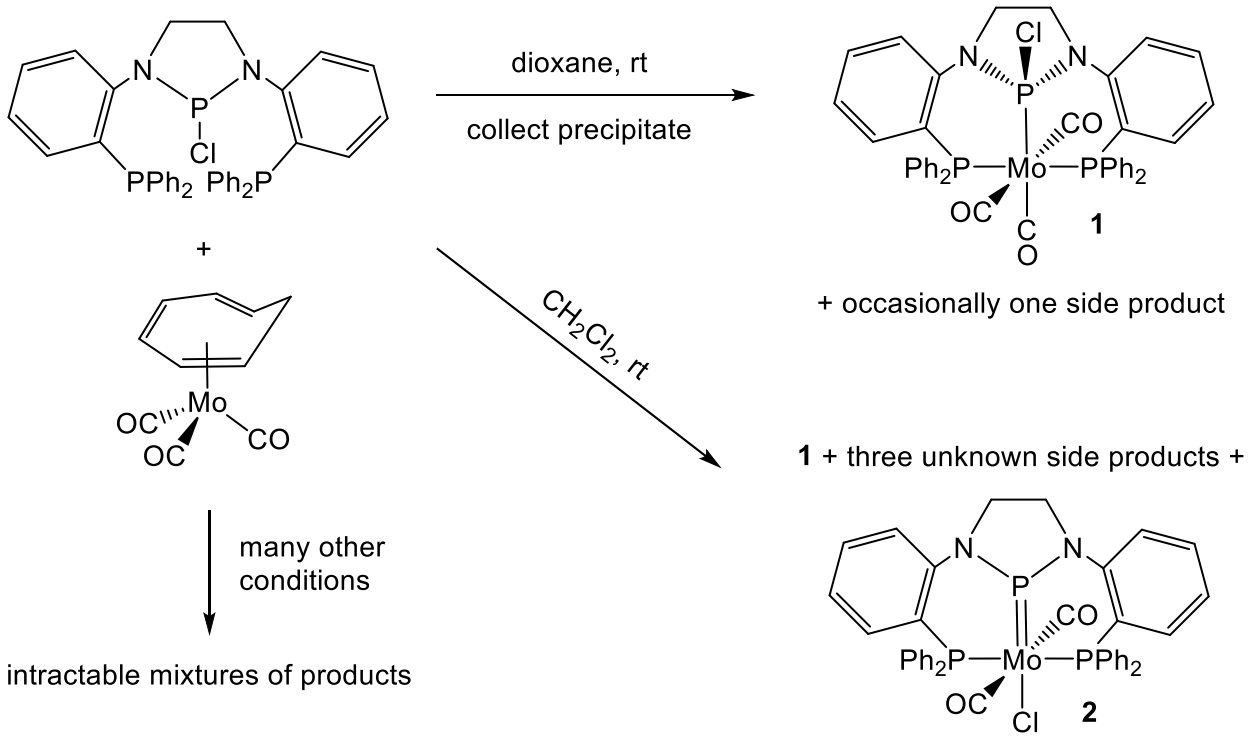

Scheme 7. Summary of coordination reactions of $(PP^{Cl}P)$ to $Mo(CO)_3$(cycloheptatriene)

To synthesize a molybdenum carbonyl complex containing a phosphenium cation, a halide abstraction route was first envisioned. In this strategy, the target molecule $(PP^{Cl}P)Mo(CO)_3$ (**1**) would hypothetically be converted to $[(PPP)Mo(CO)_3]^+$ via salt metathesis. Initially, extensive attempts to coordinate the $(PP^{Cl}P)$ ligand to $Mo(CO)_3$(cycloheptatriene) resulted in mixtures of products with similar solubilities (Table 1). Nonetheless, attempts at isolation were reinvigorated when X-ray diffraction-quality crystals of **1** were grown from a concentrated C_6D_6 solution in an NMR tube (Figure 1). **1** features an octahedral Mo atom coordinated by pincer ligand $(PP^{Cl}P)$ and three CO ligands in a meridional arrangement.

Table 1. Screening reaction conditions for the optimal synthesis of **1** or **2**

Method	Reaction conditions	^{31}P product signals >140 ppm
1	THF, rt, 16 h	170 (t), 164 (d), 151 (t), 144 (t)
2	THF, 40°C, 16 h	170 (t), 164 (d), 157 (t), 155 (t), 151 (t)
3	THF, 40°C, 2 days	170 (t), 164 (d), 151 (t)
4	THF, 55°C, 7 days	170 (t), 164 (d), 155 (d), 151 (t)
5	THF, rt, 24 h, dark	170 (t), 164 (d), 151 (t), 145 (t)
6	CH_2Cl_2, rt, 1.5 h	170 (t), 164 (d), 144 (t)
7	CH_2Cl_2, rt, 16 h	311 (t), 172 (d), 170 (t), 164 (d)
8	Dioxane, rt, 16 h	170 (t), 164 (d), 162 (t), 152 (t)
9	Dioxane, rt, 16 h (precipitate)	170 (t)
10	Dioxane, 50°C, 5 days	170 (t), 164 (d), 155 (d)
11	Dioxane, 65°C, 16 h	170 (t), 164 (d), 155 (d), 153 (t), 151 (t)
12	Dioxane, rt, 1 h, 1 min vacuum "burping" every 15 min	311 (t), 194 (d), 172 (d), 170 (t), 164 (d), 162 (t), 152 (t), 144 (t)
13	Dioxane, rt, 24 h, static vacuum	311 (t), 172 (d), 170 (t), 164 (d), 156 (d), 152 (t)
14	PhF, rt, 24 h	329 (t), 170 (t), 161 (t), 159 (t)
15	PhF, 50°C, 24 h	170 (t), 164 (d), 151 (t)
16	PhF, 50°C, 5 days	150 (t)

1 was synthesized most reliably by Method 9 (Table 1), exhibiting ^{31}P NMR resonances at 170 (t) and 31 (d) ppm. Occasionally, this method would yield a mixture containing a second product exhibiting ^{31}P NMR resonances at 155 (t) and 33 (d) ppm and a single ^{1}H NMR backbone resonance at 2.8 ppm, but the identity of this product remains unknown. For each of the other reaction conditions in Table 1, multiple additional products were observed by NMR spectroscopy, but spectroscopic data was insufficient for assigning structures to products in the mixtures besides **1**. However, crystals grown in CH_2Cl_2 at -35°C from a reaction with the conditions in Method 7 (Table 1) yielded a crystal structure of an additional unique compound, (PPP)MoCl(CO)$_2$ (**2**). **2** features an octahedrally coordinated Mo dicarbonyl with a chloride positioned *trans*- to the P^{NHP}. As a result of CO dissociation and chloride migration to the metal, this complex features a P^{NHP} bearing no substituent, indicative of either a phosphenium or

phosphido ligand. However, the planar geometry of the P^{NHP} and the shortening of the Mo-P^{NHP} bond by 0.17 Å relative to **1** (Figure 1) both suggest that the NHP is best classified as a phosphenium in **2**.

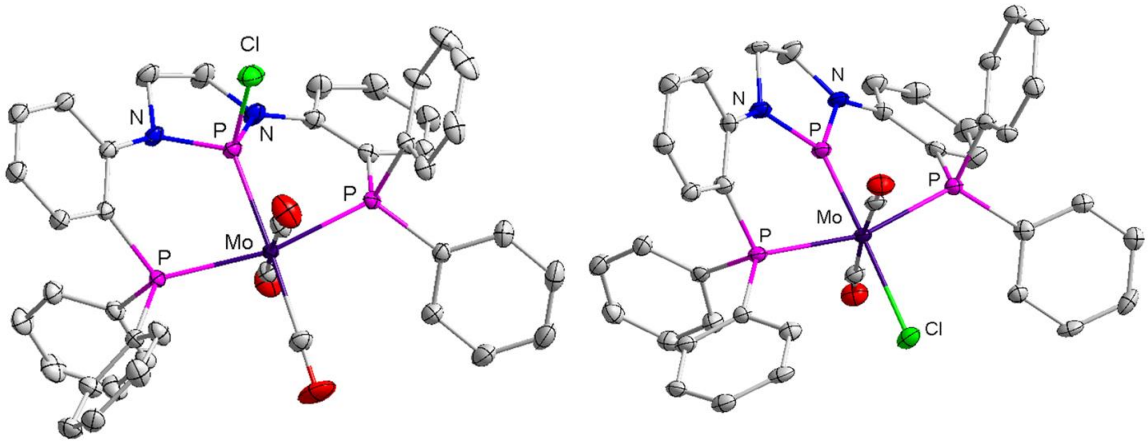

Figure 1. Crystal structures of **1** (Mo-P^{NHP} = 2.3240(3) Å) and **2** (Mo-P^{NHP} = 2.1462(16) Å)

To provide further evidence supporting this assignment, density functional theory methods were used to investigate the orbitals involved in the Mo-P^{NHP} bond. Natural bond orbital (NBO) calculations performed by Andrew Poitras for **2** using the M06 functional with the LANL2DZ/D95V basis sets revealed two NBOs, including a σ bond resulting from the phosphorus sp^2-hybridized orbital σ-donating to Mo and a π bond resulting from a molybdenum d orbital π-backbonding to phosphorus (Figure 2). The assigned directions of electron donation are supported by the fact that the σ-bonding orbital has a higher percentage of phosphorus parentage whereas the π-bonding orbital has a higher percentage of molybdenum parentage.

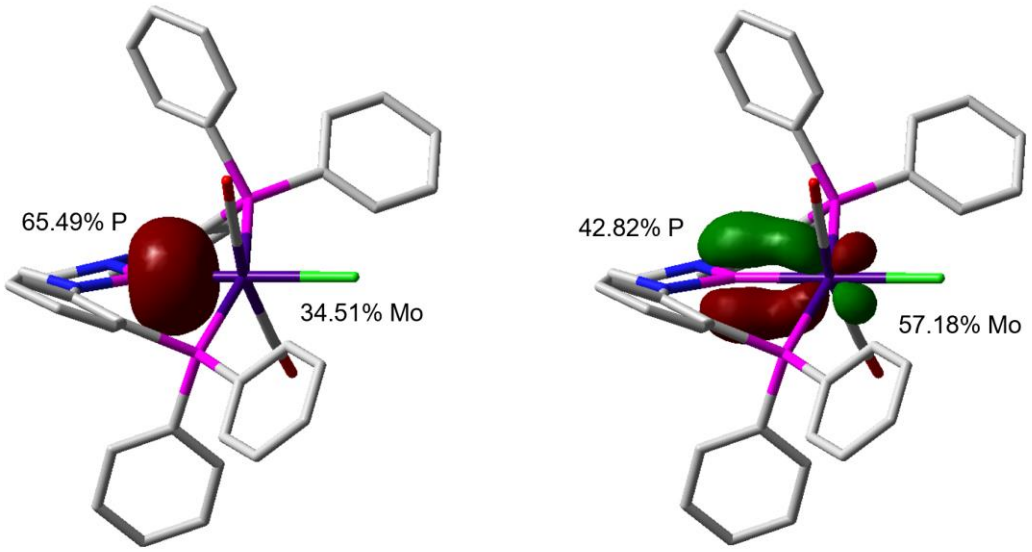

Figure 2. Pictorial representations of the two Mo-P^{NHP} natural bond orbitals calculated for **2**.

Oxidation and Reduction of $(PP^{Cl}P)Mo(CO)_3$

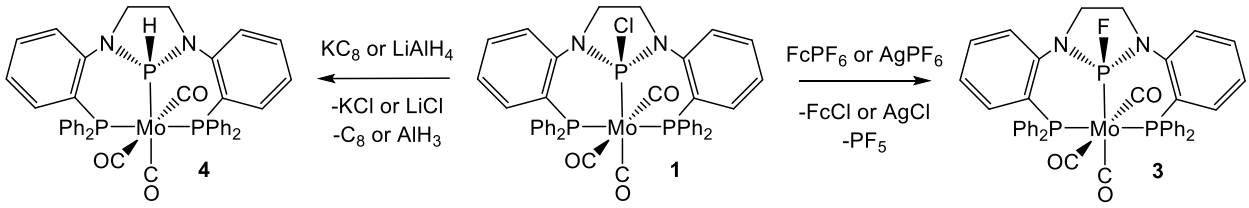

Scheme 8. Oxidation and reduction reactions of **1**

Although a crystal structure of **2** was obtained, **2**'s presumed ^{31}P NMR resonance at 311 ppm constituted ~ 1% of the product mixture. As such, this synthetic route was dismissed and the initial strategy of halide abstraction from **1** was instead pursued. Treatment of **1** with $AgPF_6$ or $FeCp_2PF_6$ both generated $(PP^FP)Mo(CO)_3$ (**3**) as the major product, as evidenced by P-F coupling in the ^{31}P NMR resonances at 162 (dt) and 47 (dd) ppm (Scheme 8). Given these observations, it is presumed that a transient phosphenium species $[(PPP)Mo(CO)_3][PF_6]$ is generated but is sufficiently reactive to break the P-F bond of the counteranion, yielding volatile

PF_5 as a byproduct. Rather than abstract the halide from the metal complex, halide abstraction before coordination of the pincer ligand was also considered. Unfortunately, the reaction between ligand salt (PPP)BPh_4 and $Mo(CO)_3$(cycloheptatriene) in dioxane yielded an intractable mixture of products, including species exhibiting multiplets (dt?) in the $^{31}P\{^1H\}$ NMR spectrum at 144 and 138 ppm.

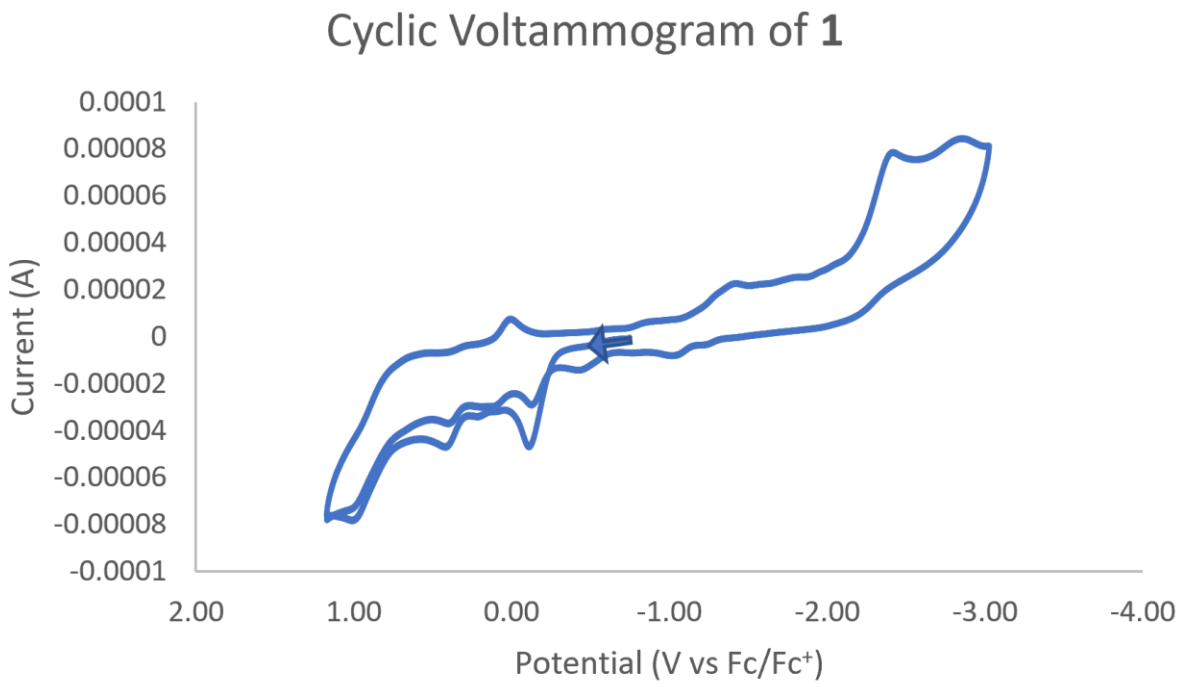

Figure 3. Cyclic voltammogram of **1** collected in THF with 0.3 M $^nBu_4NPF_6$ as a supporting electrolyte. CV parameters: scan rate = 0.3 V/s, sample interval = 0.001 V, quiet time = 2 s, sensitivity = 0.0001 A/V.

To investigate the electrochemical redox profile of **1**, cyclic voltammetry was performed in THF using $^nBu_4NPF_6$ as a supporting electrolyte (Figure 3). Although the obtained voltammogram does not display ideal "duck"-like reversible features, it does suggest that **1** is capable of undergoing both oxidation and reduction. It is worth noting that since **1** can cleave P-

F bonds upon treatment with PF_6^- salts, it is likely that under oxidizing conditions, **1** similarly reacted with the supporting electrolyte in this experiment. To complement the oxidative chemistry previously attempted, **1** was treated with KC_8 as reductant (Scheme 8). However, the observed major product was $(PP^HP)Mo(CO)_3$ (**4**), featuring ^{31}P NMR resonances at 134 (dt) and 51 (d) ppm. Crystals of **4** grown from a concentrated dioxane solution corroborate a structure analogous to **1** featuring an octahedrally coordinated Mo atom with three CO ligands arranged in a meridional fashion (Figure 4). The source of the H atom in this reaction is unknown, though it is likely from either lingering cycloheptatriene or THF solvent. Treatment of **1** with $LiAlH_4$ as an alternative reductant also yielded **4** as the major product.

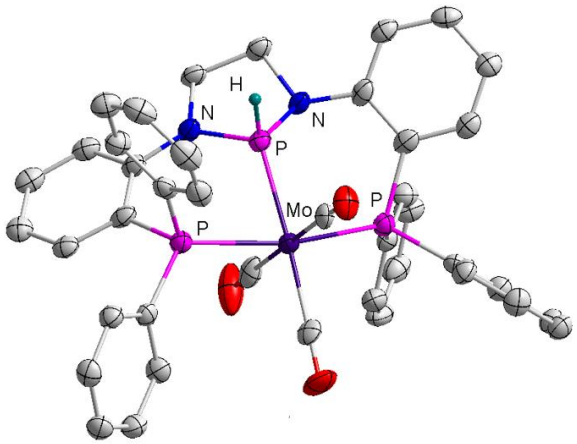

Figure 4. Solid state structure of **4** featuring a P-H bond identifiable by crystallography

Attempted Synthesis of (PPP)MoCl(CO)$_2$ by Decarbonylation

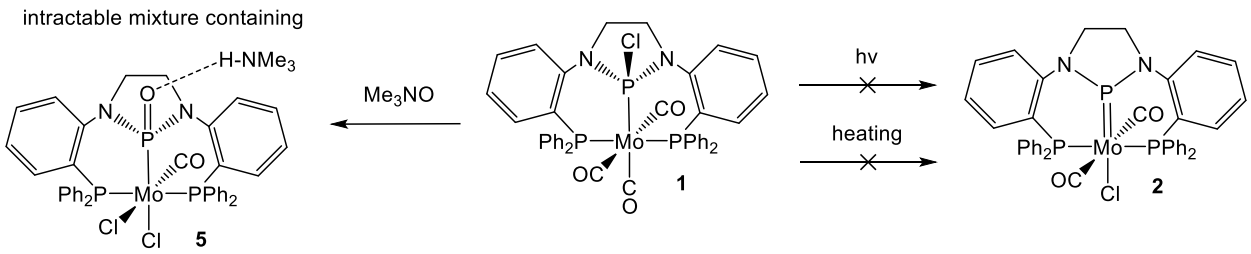

Scheme 9. Attempts at decarbonylation of **1**

Acquisition of the crystal structure of **2** provided inspiration for an alternate synthetic route to a Mo phosphenium complex: dissociation of a CO ligand and migration of the halide from P^{NHP} to Mo. Traditional methods for encouraging removal of CO ligands include thermolysis, photolysis, and O-atom donor reagents. Thermolysis of **1** in a wide range of reaction conditions had already been attempted repeatedly (Table 1) without success. Applying vacuum during the reaction generated intractable mixtures, though a phosphenium species was observed as one component (Table 1). Irradiation experiments were also attempted under a variety of conditions including white light, blue light, and 254 nm light, but none generated a phosphenium complex observable by ^{31}P NMR spectroscopy.

Next, atom-transfer oxidation reagents were employed in attempts to oxidize CO to the excellent leaving group CO_2. **1** was treated with both Me_3NO and pyridine-N-oxide as O-atom donors. Both reactions resulted in intractable mixtures of products, neither of which exhibited downfield ^{31}P NMR signals characteristic of a phosphorus atom with an open coordination site. Purple needle crystals suitable for X-ray diffraction were grown from slow evaporation of diethyl ether into a THF solution of the Me_3NO reaction. Disappointingly, this yielded a structure of $[(PP^{O}P)MoCl_2(CO)][HNMe_3]$ (**5**) in which the trimethylammonium proton hydrogen-bonds to the phosphorus oxide. Although carbonyl ligands were removed and chlorides migrated, **5** is an undesirable product because of the formation of an inert P=O bond. As P is an oxophilic element, it is unsurprising that the donated O atom was not selective for CO ligands. The source of the trimethylammonium proton is presumably adventitious water since both Me_3NO and pyridine-N-oxide are notoriously hygroscopic.[118]

Decarbonylation of (PP^{I}P)Mo(CO)$_3$

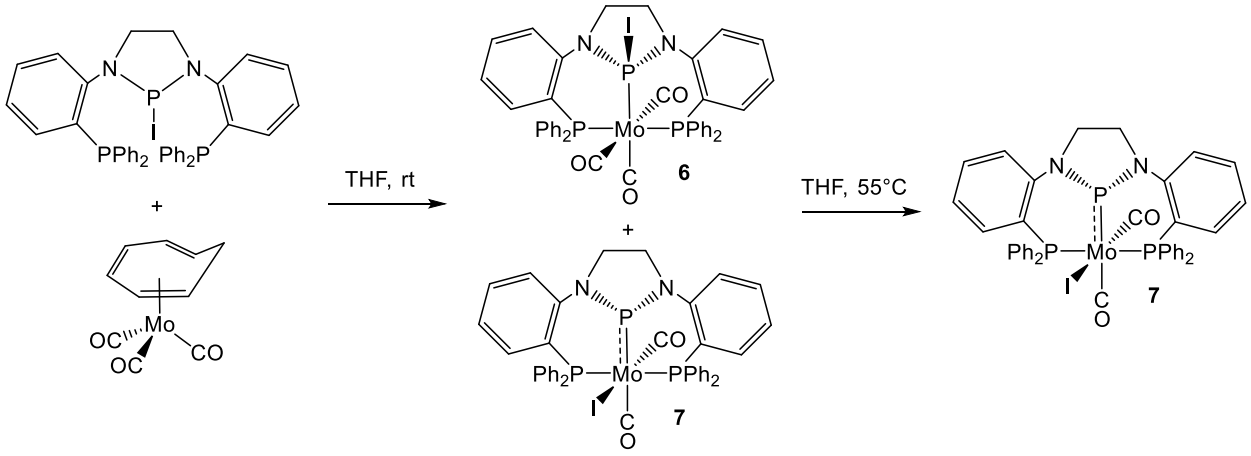

Scheme 10. Synthesis and decarbonylation of iodophosphine complex

After numerous attempts to force chloride migration by dissociation of a carbonyl, attention was turned to a larger halophosphine substituent, iodine. Since P-I bonds are weaker than P-Cl bonds, it was hypothesized that halide dissociation and migration to Mo may be more facile for iodide than chloride in polar aprotic solvent. Treatment of Mo(CO)$_3$(cycloheptatriene) with (PP^{I}P) ligand in THF overnight yielded two products with drastically different NHP chemical shifts. The product with ^{31}P resonances at 160 (t) and 34 (d) ppm was assigned as (PP^{I}P)Mo(CO)$_3$ (**6**) while the product with resonances at 326 (t) and 18 (d) ppm was assigned as the decarbonylated product (PPP)MoI(CO)$_2$ (**7**). It is noteworthy that partial conversion was achieved without the use of additional heating or UV irradiation. Indeed, full conversion of **6** to **7** can be achieved by heating above 50°C. Surprisingly, ^{1}H NMR signals for **7** were observed at 3.87 and 3.07 ppm, suggesting that the protons of the N-heterocycle's ethylene backbone are diastereotopic. This is evidence that **7**'s NHP has a pyramidal coordination geometry and that **7** is therefore not isostructural to **2**. In the absence of a solid state structure or XANES data, it is ambiguous whether **7** is best electronically described as NHP^{+}/Mo^{0} or NHP^{-}/Mo^{2+}; in Enemark-

Feltham notation, the M-NHP moiety can be described as {Mo-P}^{6}. Regardless, **7** is the compound in this work most likely to be capable of σ bond activation or catalytic activity; the complex has a vacant coordination site at P^{NHP} and a second can be generated at Mo upon iodide dissociation.

Reactivity of $(PP^{H}P)Mo(CO)_3$

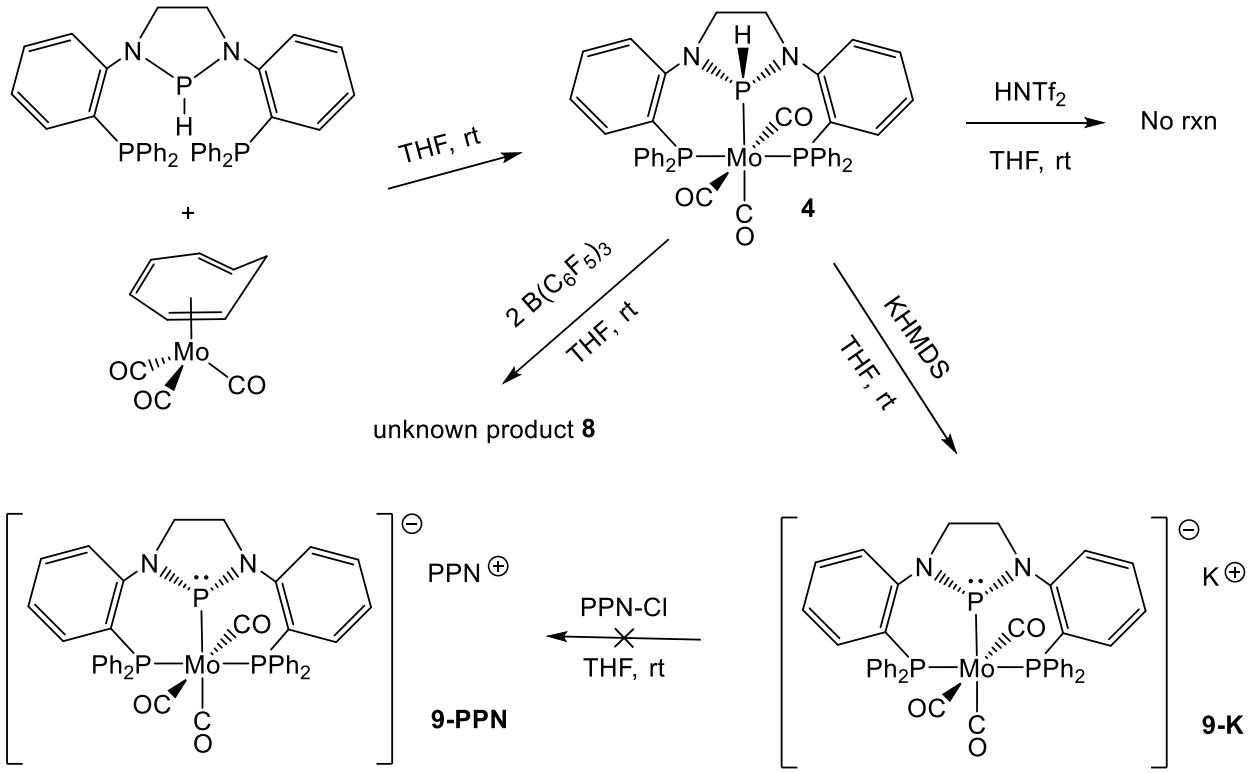

Scheme 11. Synthesis and reactivity of phosphine complex **4**

Although **4** could be synthesized by reduction of **1**, the overall yield was found to be significantly greater if the reduced ligand ($PP^{H}P$) was coordinated to $Mo(CO)_3$(cycloheptatriene) instead. Unlike the ($PP^{Cl}P$) coordination reaction, the ($PP^{H}P$) coordination reaction in THF did not yield multiple products. In addition to the more facile synthesis, **4** was of greater interest than **1** due to the potential for acidic and/or hydridic behavior of the P-H moiety.

Since previous unpublished work by Andrew Poitras and Leah Oliemuller on (PP^HP) Co and Ni complexes each suggested that the P-H moiety was hydridic rather than acidic, studies of **4** began by similarly exploring hydricity. First, **4** was treated with the Brønsted acid $HNTf_2$ in hopes of using a proton to remove a P-H hydride, generating H_2 and a phosphenium complex. However, no color change or gas evolution was observed after stirring overnight in THF and NMR data indicate no reaction. Next, attention was turned to reactivity with the Lewis acid $B(C_6F_5)_3$, again in hopes of removing a hydride. Surprisingly, treatment of **4** with one equivalent of $B(C_6F_5)_3$ in THF generated a 1:1 mixture of **4** and unknown product **8** with ^{31}P resonances at 149 (t) and 48 (d) ppm. Addition of a second equivalent of $B(C_6F_5)_3$ resulted in full conversion to the product. Although **8**'s identity remains unknown, ^{31}P spectroscopic data can eliminate a few possibilities. The product's NHP resonance is not sufficiently downfield to be a phosphenium or phosphido complex. Additionally, the lack of P-H coupling indicates that the product does not feature a hydride bridging the NHP and $B(C_6F_5)_3$. Similarly, no P-F coupling is observed. The current hypothesis is that a P-Ar^F bond is formed as the results of P-C bond cleavage.

To complement **4**'s hydridic activity, its acidity was next probed. Treatment of **4** with KHMDS in THF resulted in an immediate color change to bright red, yielding $[(PPP)Mo(CO)_3]K$ (**9-K**). Since salt **9-K** was insoluble in C_6D_6 and would likely react with $CDCl_3$, ^1H NMR data could not be obtained. However, **9-K** displayed ^{31}P NMR resonances at 349 and 57 ppm in THF, supporting the assignment of an empty coordination site on the NHP. It is extremely likely that **9-K** is best described as NHP^-/Mo^0 rather than NHP^+/Mo^{2-} because the Mo^{2-} oxidation state is extremely uncommon. In an attempt to provide more evidence for the phosphido description by observing diastereotopic protons in the ^1H NMR spectrum, a salt metathesis reaction was performed to generate a salt with a large organic cation. However, upon treatment of **9-K** with

PPN-Cl, **9-PPN** was not generated. Instead, the product mixture yielded a NMR spectrum including **4** but no ^{31}P resonances downfield of 150 ppm. Alternatively, ^{1}H NMR data for **9-K** could be collected in deuterated THF in the future.

Higher Valent Complexes: $MoCl_3$ instead of $Mo(CO)_3$ Fragment

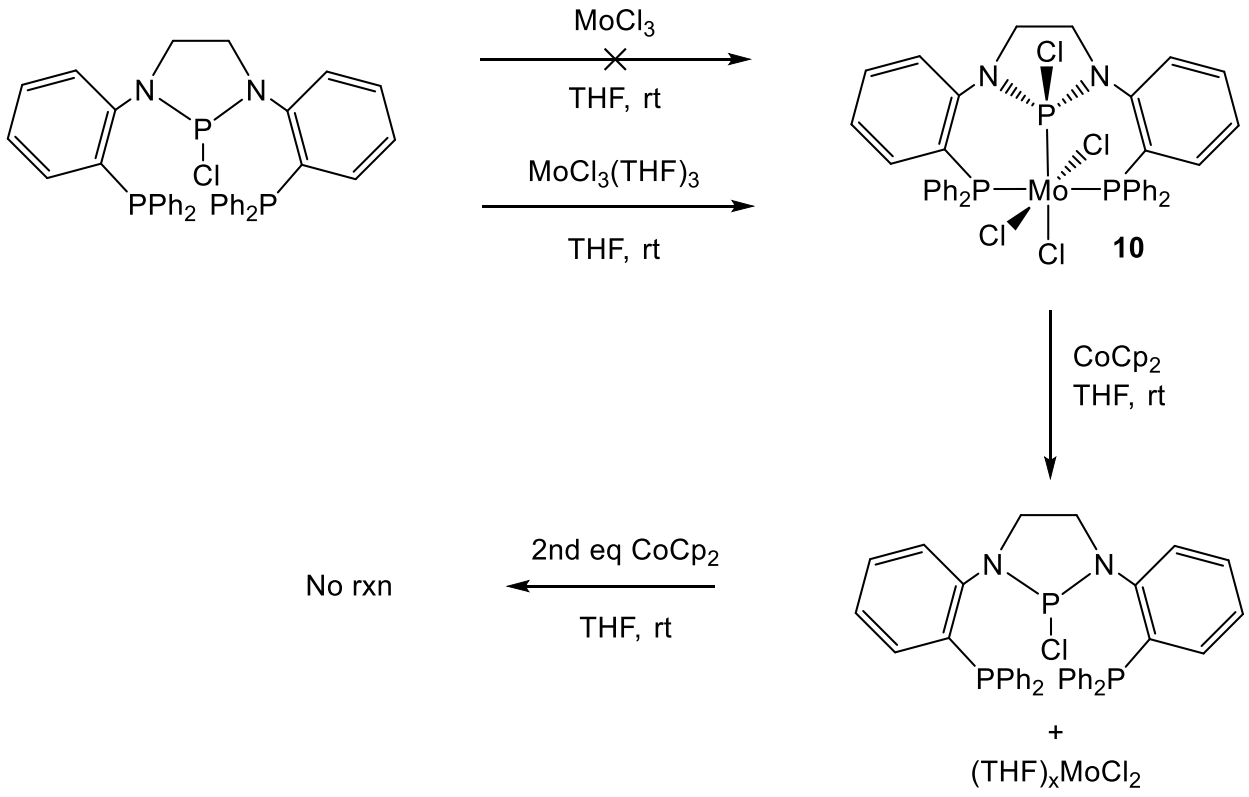

Scheme 12. Synthesis of Mo^{3+} complex

Although the synthesis of numerous NHP-Mo compounds has been described throughout this work, most of them are unlikely to display catalytic activity because they are coordinatively saturated. Ligand dissociation to vacate a coordination site at Mo is ideal if reactivity is to be studied, but carbonyl ligands are difficult to remove. To combat this problem, complexes containing or derived from a $MoCl_3$ fragment were envisioned. Initial studies began by

attempting to coordinate the ($PP^{Cl}P$) ligand directly to $MoCl_3$ in THF, but the product mixture contained primarily free ($PP^{Cl}P$) with little to no paramagnetic product. This is likely due to the large amount of energy required to disrupt the salt's ionic lattice and coordinate the pincer ligand.

To combat this problem, $MoCl_3(THF)_3$ was prepared by a literature procedure and instead utilized as a metal precursor.[119] Coordination of ($PP^{Cl}P$) to purple $MoCl_3(THF)_3$ yielded a paramagnetic yellow-brown product displaying ^{1}H NMR resonances within the 0-12 ppm range. Although a crystal structure remains unobtained, it is likely that this complex is ($PP^{Cl}P$)$MoCl_3$ (**10**). In the literature, pincer Mo trihalide complexes are often treated with three equivalents of reductant to remove all halides, yielding a coordinatively unsaturated, low-valent Mo complex. Such complexes frequently bind N_2, dimerizing around it and/or cleaving it into two Mo nitrides that can be reduced to ammonia.[102–105,120] For **10**, it was hypothesized that similar reactivity may occur, though the presence of the fourth halide bound to the central phosphorus may complicate the chemistry. Treatment of **10** with one equivalent of $CoCp_2$ as a mild reductant in THF generated a muddy brown mixture within minutes. ^{1}H NMR data indicated that the product was primarily composed of free ligand ($PP^{Cl}P$) with minor paramagnetic impurities. This suggests that the metal was ejected from the pincer complex upon reduction to Mo^{2+}. Treatment with an additional equivalent of $CoCp_2$ resulted in no further reaction, as evidenced by the major $CoCp_2$ ^{1}H NMR resonance at -45 ppm.

Computational Investigation of (PP^XP)$Mo(CO)_3$ Isomers and Derived Products

Since ^{1}H NMR data suggest that **7** is not isostructural to **2**, computational methods were utilized to investigate whether such complexes are more stable when the halide is *trans*- to a CO

or the NHP. In addition, the mechanism of CO dissociation and halide migration was of interest. A few dissociative pathways were considered for this experiment. First, X^- could dissociate from $(PP^XP)Mo(CO)_3$ and go outer-sphere, yielding X^- and $[(PPP)Mo(CO)_3]^+$. Next, a CO could dissociate from the complex; however, with multiple carbonyls, this could happen either from the position *cis*- or *trans*- to the NHP unit. This would yield X^-, CO, and *cis*- or *trans*-vacant $[(PPP)Mo(CO)_2]^+$. From here, X^- could bond to the metal, either in a *cis*- or *trans*- position relative to the NHP. Given that *trans*-$(PPP)MoCl(CO)_2$ (**2**) has been structurally characterized, it was hypothesized that either Cl^- binds in the *trans*- position or it binds in the *cis*- position and subsequently isomerizes to *trans*-. An alternative pathway could involve initial dissociation of a CO ligand rather than X^-, yielding a $(PP^XP)Mo(CO)_2$ intermediate. However, later intermediates in this pathway would be the same as those listed in the previous pathway. These pathways would contrast with the iodide analogue, since ^{1}H NMR data suggest **7**'s halide is *cis*- to the NHP.

Geometry optimization and vibrational frequency calculations were performed on the following species in the gas phase: $(PP^XP)Mo(CO)_3$, $[(PPP)Mo(CO)_3]^+$, *cis*-vacant $[(PPP)Mo(CO)_2]^+$, *trans*-vacant $[(PPP)Mo(CO)_2]^+$, *cis*-$(PPP)MoX(CO)_2$, *trans*-$(PPP)MoX(CO)_2$, *trans*-vacant $(PP^XP)Mo(CO)_2$, *cis*-vacant $(PP^XP)Mo(CO)_2$ "A", *trans*-vacant $(PP^XP)Mo(CO)_2$ "B", X^-, and CO for X = H, F, Cl, Br, and I (Chart 1). All calculations were performed using the M06 functional[119] with LANL2DZ basis set for Mo, Cl, and Br, LANL2DZ(d,p) for I, and D95 for C, H, O, N, and F. Input geometries were constructed beginning from the crystal structures of **1**, **2**, and **4**. All starting geometries retained the octahedral coordination environment or octahedral with one vacancy. When changing X substituents, Mo-X or P-X bonds were adjusted accordingly for the input geometry based on the sum of the elements' covalent radii. Optimized

geometries were inspected to confirm that all calculated vibrational frequencies were real numbers. All calculations attempted using LANL2DZ instead of LANDL2DZ(d,p) for I either failed to converge or yielded nonsensical geometries. Energies of species within each intermediate step were summed to calculate the energy of the system in each of those configurations. Finally, energies for each -X substituent were normalized such that the lowest energy species or collection of species was set to 0 kJ/mol. Energies for each of the considered species or collections of species are tabulated in Table 2.

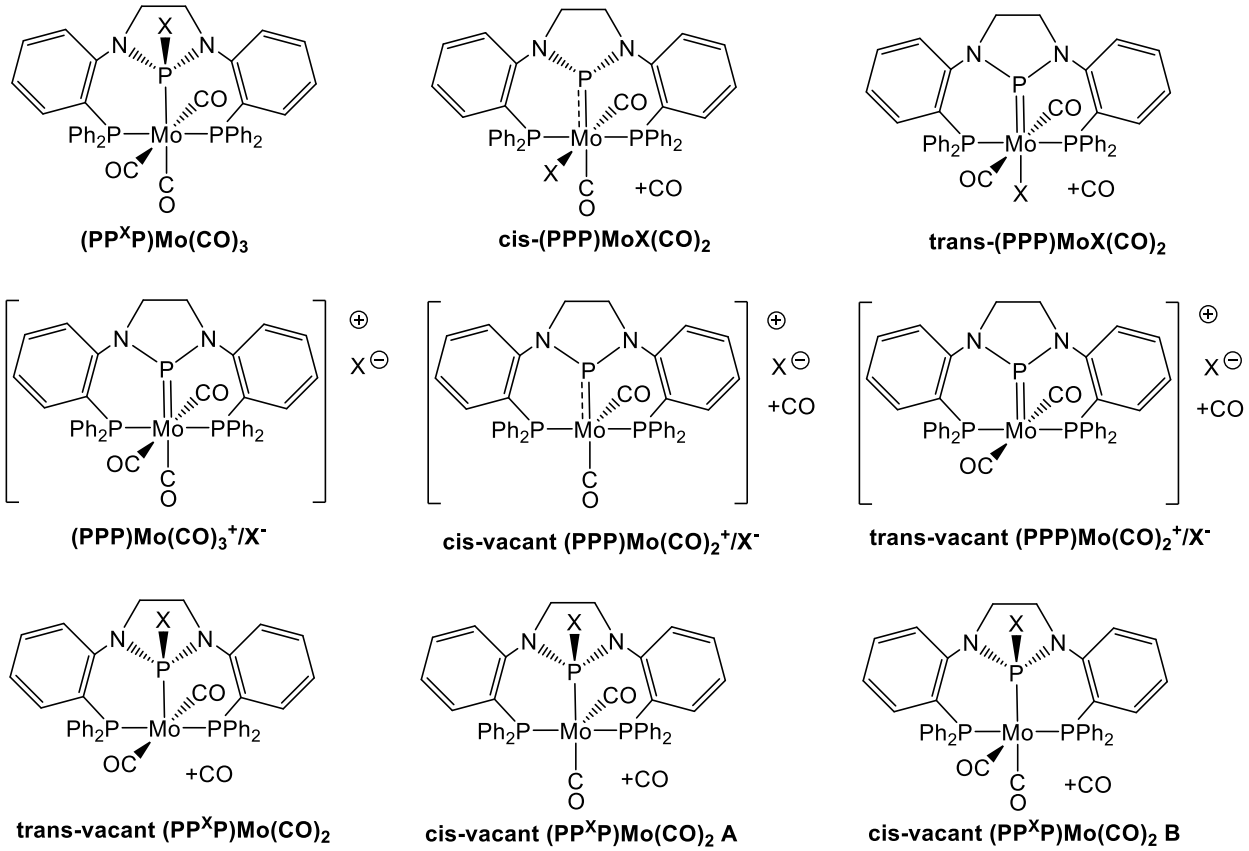

Chart 1. Species examined in this study

Table 2. Calculated free energies for each species or sum of species

Species	X=H	X=F	X=Cl	X=Br	X = I
$(PP^XP)Mo(CO)_3$	0.0000000	0.0000000	0.0000000	0.0000000	0.0000000
$[(PPP)Mo(CO)_3]^+$ plus X^-	886.2559035	649.5119430	469.2162325	424.8137765	407.6456320
***cis*-vacant $[(PPP)Mo(CO)_2]^+$ plus X^- plus CO**	1024.5304865	787.7865260	607.4908155	563.0883595	545.9202150
***trans*-vacant $[(PPP)Mo(CO)_2]^+$ plus X^- plus CO**	1037.9074090	801.1634485	620.8677380	576.4652820	559.2971375
***cis*-$(PPP)MoX(CO)_2$ plus CO**	172.4192105	112.7809780	74.5878295	83.7298205	99.1730115
***trans*-$(PPP)MoX(CO)_2$ plus CO**	171.3453810	135.5073060	83.0524415	86.7832770	97.0673605
$(PP^XP)Mo(CO)_2$ plus CO	191.1757825	193.3496965	152.4365300	153.8070410	143.2630330

For most -X substituents, only one or two of the isomers *trans*-vacant $(PP^XP)Mo(CO)_2$, *cis*-vacant $(PP^XP)Mo(CO)_2$ A, and *trans*-vacant $(PP^XP)Mo(CO)_2$ B optimized to a minimum. As such, the three are combined as $(PP^XP)Mo(CO)_2$ in Table 2 and the lowest energy found is reported. From these calculations, the most glaring trend is that species containing cation/anion pairs are significantly greater in energy than the neutral complexes. This is likely due to the fact that all energies were calculated in the gas phase for individual molecules and ions. This method ignores the stabilizing effects of intermolecular interactions and solvent effects (*vide infra*). Another takeaway is that $(PP^XP)Mo(CO)_2$ species are higher in energy than their $(PPP)MoX(CO)_2$ isomers. This is expected given the synthetically observed halide migration and the fact that $(PP^XP)Mo(CO)_2$ is a 16-electron complex whereas $(PPP)MoX(CO)_2$ is an 18-electron complex.

Findings from these calculations regarding *cis*-vacant vs. *trans*-vacant $(PPP)MoX(CO)_2$ are troubling as they do not match well with data collected in the laboratory. For X = F, Cl, and

Br, the *cis*- isomer is calculated to be more stable than the *trans*- isomer. This is consistent with the fact that *cis*-vacant (PPP)Mo(CO)$_2^+$ was calculated to be lower in energy than *trans*-vacant (PPP)Mo(CO)$_2^+$ but is not consistent with the fact that the crystal structure obtained for **2** features a halide *trans*- to the NHP. For X = H, the *trans*- isomer is more stable, but this analogue is not directly comparable because the hydride ligand is small and significant distortion from an octahedral geometry is observed. However, for X = I, the *trans*- isomer is also calculated to be more stable. This is inconsistent with the analogues containing other halides as well as the fact that ^{1}H NMR data suggest that **7**'s NHP has a pyramidal coordination geometry.

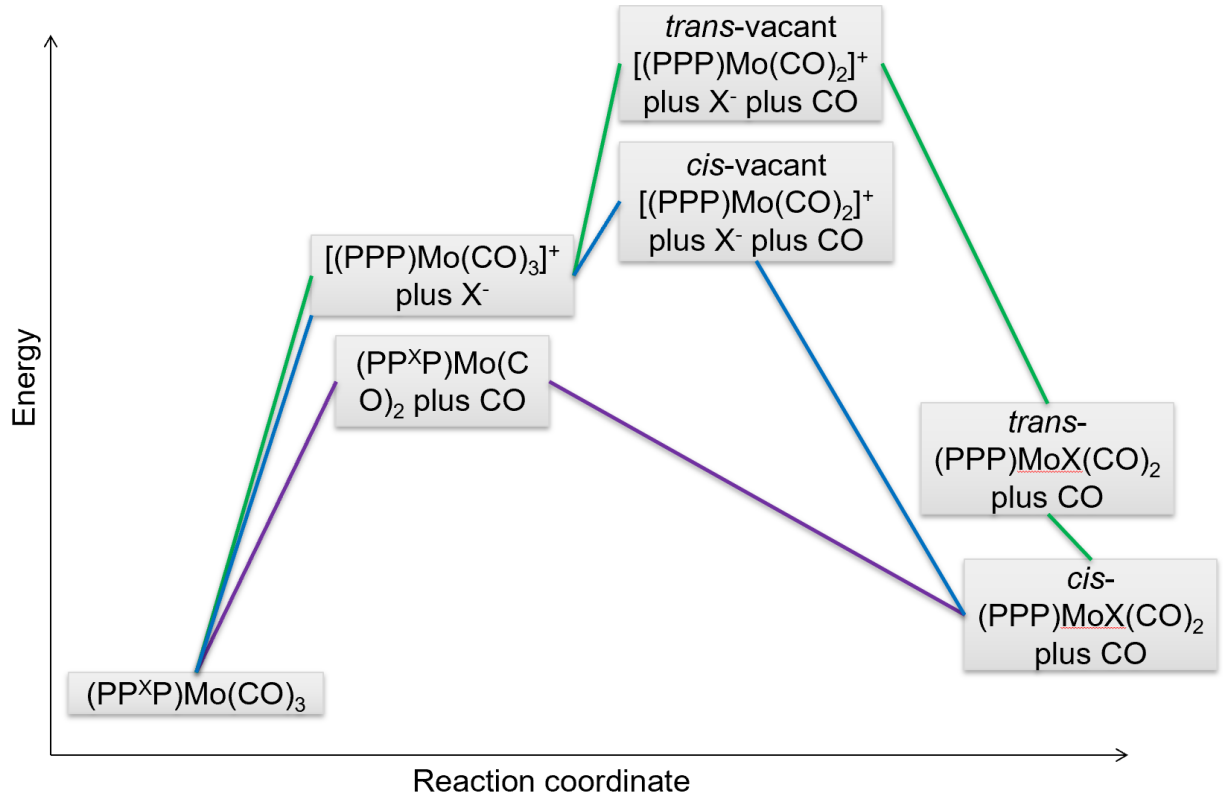

Figure 5. Generalized reaction coordinate diagram showing a few possible mechanistic pathways for reaching final the product with X = F, Cl, or Br. Note that relative order of energies is displayed qualitatively rather than quantitatively; actual energy differences vary highly.

Data for X = F, Cl, and Br were used to generate a qualitative reaction coordinate diagram (Figure 5). The lowest-energy path to a decarbonylated product would involve CO dissociation from the position *cis*- to the NHP as the first step. Next, the halide would dissociate from the NHP, but it is likely that the halide always remains inner-sphere since it migrates from the NHP to the adjacent vacant coordination site on Mo. These steps may also be concerted, but this could only be probed by transition state calculations.

Given the great disparity in energy found between neutral and ionic complexes (Table 2), additional calculations were performed using a THF solvation model. Geometry optimization and vibrational frequency calculations were performed using the optimized geometries from the gas phase as input geometries. However, multiple calculations inexplicably failed to converge despite converging for the gas phase calculations. Data for X = H, F, Br, and I are the most complete and are tabulated in Table 3.

Table 3. Calculated free energies for each species or sum of species with THF solvation

Species	X=H	X=F	X=Br	X=I
$(PP^XP)Mo(CO)_3$	0.0000000	0.0000000	0.0000000	0.0000000
$[(PPP)Mo(CO)_3]^+$ plus X^-	364.5296710	218.7829150	132.8949335	65.1176510
***cis*-vacant** $[(PPP)Mo(CO)_2]^+$ **plus** X^- **plus CO**	462.9964230	317.2496670	231.3616855	163.5844030
***trans*-vacant** $[(PPP)Mo(CO)_2]^+$ **plus** X^- **plus CO**	483.5383350	337.7915790	251.9035975	184.1263150
***cis*-** $(PPP)MoX(CO)_2$ **plus CO**	160.0924880	111.5207380	93.3207720	78.6022190
***trans*-** $(PPP)MoX(CO)_2$ **plus CO**	179.8073675	132.7715350	94.5153745	Failed to converge

Some interesting conclusions can be drawn from the simulated solvent data. Most notably, ionic complexes are significantly stabilized relative to the gas phase calculations: $(PPP)Mo(CO)_3^+/X^-$ is only 65-364 kJ/mol greater in energy than $(PP^XP)Mo(CO)_3$ rather than 408-886 kJ/mol. Furthermore, for X = I, $(PPP)Mo(CO)_3^+/X^-$ is more stable than the product *cis*-$(PPP)MoX(CO)_2$. This is the case only for X = I and suggests that the lability of the iodide ion in polar solvent is indeed responsible for direct conversion of $(PP^IP)Mo(CO)_3$ to $(PPP)MoI(CO)_2$ synthetically. Attempted calculations for $(PP^XP)Mo(CO)_2$ consistently failed to converge, leaving unknown whether iodide or CO dissociation occurs first mechanistically.

Conclusion

The coordination chemistry of (PP^XP) pincer ligands to $Mo(CO)_3$ and $MoCl_3$ fragments has been explored synthetically. Although $(PP^{Cl}P)$ is not incompatible with $Mo(CO)_3$, isolating pure products in good yield remains a challenge. Furthermore, attempts to remove the chloride failed to generate an isolable phosphenium complex in quantitative yield. Similarly, chemistry of higher valent analogues does not seem promising due to complex decomposition. Alternatively, coordination of the (PP^IP) ligand to $Mo(CO)_3$ results in direct conversion to **7**, a compound which has enough available coordination sites to accommodate σ bond activation and potentially catalysis. The exact electronic description of **7** remains unknown despite computational investigations, as does the mechanism for its formation from **6**. Syntheses of complexes using the (PP^HP) ligand are the most facile, and subsequent reactivity studies demonstrate the ligand's ambiphilic character and propensity for redox non-innocence.

Outlook

The future of this project will likely be centered around **7**'s reactivity. Treatment with MeI would be an interesting experiment: would the NHP act as a nucleophile to form a P-Me bond or as an electrophile to form a P-I bond? Additionally, reactivity with substrates containing polar E-H bonds should be screened. Studies should begin with an acidic E-H bond like phenol or thiophenol; if **7** or a derivative with an outer-sphere anion can't cleave the weak E-H bond of these substrates, this system has little to no potential for σ bond activation. If the complex is capable of activating such bonds, stronger or less polar E-H bonds should be subsequently tested.

Although the ($PP^{H}P$) system doesn't have as many available coordination sites, it may have use in some of the reactivity described in the Introduction for free NHP or NHP-H molecules. At the very least, it is an excellent case study verifying the ($PP^{NHP}P$) ligand's utility as a redox non-innocent ligand. Additionally, it may be prudent to determine the IR $\nu_{P\text{-}H}$ of **4**, as this value is reported for numerous other characterized NHP-H complexes. Although the stretching frequency was indeterminable due to multiple peaks present in the P-H region of the IR spectrum, an isotopic labelling study using ($PP^{D}P$) could elucidate the stretching frequency.

The outlook for the ($PP^{Cl}P$) system is less optimistic. Synthesis and isolation of **1** remains difficult despite extensive reaction condition screening. However, it may be interesting to see if treatment of **1** with $NaBPh_4$ generates a stable tricarbonyl phosphenium complex with an outer-sphere cation.

Experimental

General Considerations. All reported reactions were carried out on a Schlenk line or in a nitrogen atmosphere glovebox in the absence of water or dioxygen. All bulk solvents were

degassed and dried via passage through columns of drying agents using a Seca solvent purification system from Pure Process Technologies, then stored in the glovebox over 3 Å molecular sieves. C_6D_6 was degassed via repeated freeze-pump-thaw cycles and stored in the glovebox over 3 Å molecular sieves. NMR data were collected at room temperature using a Bruker DPX 400 MHz or Bruker 600 MHz Avance III HD instrument. ^{1}H and ^{13}C NMR shifts were referenced to residual solvent peaks, and all ^{31}P NMR shifts were referenced to an external standard of 85% H_3PO_4. Reactants and bench solvents were purchased from Aldrich, Strem, or Alfa Aesar and used without further purification. IR spectra were recorded on a Varian 640-IR spectrometer controlled by Resolutions Pro software.

Synthesis of ($PP^{X}P$) ligands. Ligand ($PP^{Cl}P$) was synthesized in accordance with a literature procedure.[28] Ligand ($PP^{I}P$) was synthesized analogously using PI_3 instead of PCl_3, although additional toluene extractions were performed for purification due to the increased solubility of byproduct $[Et_4N][I]$ relative to $[Et_4N][Cl]$. Ligand ($PP^{H}P$) was synthesized in accordance with a forthcoming literature procedure involving reduction of ($PP^{Cl}P$) with KEt_3BH in THF.[121]

Synthesis of $MoCl_3(THF)_3$. Metal precursor $MoCl_3(THF)_3$ was synthesized in accordance with a literature procedure.[119] Notably, the product's color was purple rather than pale-orange as reported in the literature.

Synthesis of ($PP^{Cl}P$)$Mo(CO)_3$ (1). $Mo(CO)_3(C_7H_8)$ (0.018 g, 0.066 mmol) was dissolved in 1,4-dioxane (6 mL) and added to ligand ($PP^{Cl}P$) (0.043 g, 0.067 mmol). This red suspension was stirred at room temperature for 16 hours. The resulting cloudy peach/brown suspension was

filtered over a frit to isolate a peach solid. This solid was recollected in benzene and lyophilized, then solvent was removed *in vacuo* to yield **1** as a peach powder (35%, 0.019 g). Yellow crystals suitable for X-ray diffraction were grown from a concentrated C_6D_6 solution in an NMR tube. $^{31}P\{^1H\}$ NMR (161.8 MHz, C_6D_6): δ 170.2 (t, P^{NHP}, $^2J_{P\text{-}P}$ = 33.5 Hz, 1P), 30.8 (d, PPh_2, $^2J_{P\text{-}P}$ = 33.5 Hz, 2P). IR (DCM, cm^{-1}): 1968 ($\nu_{C\text{-}O}$), 1929 ($\nu_{C\text{-}O}$), 1859 ($\nu_{C\text{-}O}$).

Synthesis of mixture containing (PPP)MoCl(CO)$_2$ (2). $Mo(CO)_3(C_7H_8)$ (0.512 g, 0.188 mmol) was dissolved in DCM (6 mL) and added to ligand ($PP^{Cl}P$) (0.122 g, 0.189 mmol). This dark red solution was stirred at room temperature for 1.5 hours; no further color change was noted. Solvent was removed *in vacuo*. Orange needle-shaped crystals suitable for X-ray diffraction were grown from a concentrated DCM solution at -35°C, though crystal growth was also observed from the same solution at room temperature. The crystal structure obtained is thought to represent only a minor component of the product mixture.

Synthesis of (PP^FP)Mo(CO)$_3$ (3). <u>Method 1 (better yield and purity):</u> $AgPF_6$ (0.006 g, 0.02 mmol) was dissolved in PhF (8 mL) and added to **1** (0.020 g, 0.025 mmol). This reaction should not be run in THF, as $AgPF_6$ polymerizes THF into a solid. The resulting dark orange solution was stirred for 3 days at room temperature. After stirring, the solution was yellow-brown. Filtration over a filter pipette yielded a translucent yellow solution from which solvent was removed *in vacuo*. ^{31}P NMR (161.8 MHz, C_6D_6): δ 161.6 (dt, P^{NHP}, $^1J_{P\text{-}F}$ = 1094 Hz, $^2J_{P\text{-}P}$ = 49.8 Hz, 1P), 46.7 (dd, PPh_2, $^2J_{P\text{-}F}$ = 9.0 Hz, 2P). <u>Method 2:</u> $FeCp_2$ (0.007 g, 0.02 mmol) was dissolved in THF (4 mL) and added to **1** (0.017 g, 0.020 mmol). After stirring overnight, the yellow-orange solution was filtered over a filter pipette to collect a solution of approximately the

same color. Solvent was removed in *vacuo*. The major product is **3**. Minor product: ^{31}P NMR (161.8 MHz, $CDCl_3$): δ 40.3 (d).

Synthesis of (PP^HP)Mo(CO)$_3$ (4). $Mo(CO)_3(C_7H_8)$ (0.035 g, 0.128 mmol) was dissolved in THF (6 mL) and added to ligand (PP^HP) (0.077 g, 0.127 mmol). This red/orange solution was stirred for 16 hours at room temperature. Solvent was removed *in vacuo* from the resulting dark red/orange solution. This film was rinsed with hexanes (4 mL), then solvent was dried *in vacuo* to yield **2** as a yellow powder (94%, 0.094 g). Yellow X-ray quality crystals were grown from a concentrated 1,4-dioxane solution. ^{1}H NMR (400 MHz, C_6D_6): δ 7.72, (m, Ar-H, 8H), 6.96 (d, P-H, 1H; left peak of the doublet is observable at 7.36 ppm but right peak is obscured by aryls), 7.10 (t, Ar-H, 8H), 7.08-6.96 (m, Ar-H, 6H), 6.85 (t, Ar-H, 2H), 6.56-6.50 (m, Ar-H, 4H), 2.99 (s, CH_2, 2H), 2.77 (s, CH_2, 2H). ^{31}P NMR (161.8 MHz, C_6D_6): δ 134.1 (dt, P^{NHP}, $^1J_{P\text{-}H}$ = 322.8 Hz, $^2J_{P\text{-}P}$ = 38.1 Hz, 1P), 50.5 (d, PPh_2, $^2J_{P\text{-}P}$ = 37.0 Hz, 2P). ^{13}C NMR (150.9 MHz, THF): δ 216.0 (m, CO), 211.3 (m, CO), 148.6 (m), 139.2 (dm, $J_{C\text{-}P}$ = 38.5 Hz), 134.2 (two overlapping d, $J_{C\text{-}P}$ = 13.1 Hz), 133.8 (two overlapping d, $J_{C\text{-}P}$ = 14.0 Hz), 132.9 (s), 131.5 (s), 129.7 (d, $J_{C\text{-}P}$ = 28.1 Hz), 128.6 (d, $J_{C\text{-}P}$ = 17.6 Hz), 120.9 (s), 117.0 (s), 49.3 (s, CH_2CH_2). IR (DCM, cm^{-1}): 1978 ($\nu_{C\text{-}O}$), 1958 ($\nu_{C\text{-}O}$), 1874 ($\nu_{C\text{-}O}$).

Treatment of 1 with Me_3NO to generate a mixture containing [(PP^OP)$MoCl_2$(CO)][$HNMe_3$] (5). Me_3NO (0.002 g, 0.023 mmol) was dissolved in THF (4 mL) and added to **1** (0.019 g, 0.023 mmol). This cloudy dark orange solution turned translucent within 15 minutes and was stirred for 16 hours at room temperature. Solvent was removed *in vacuo* from the resulting solution. ^{31}P NMR (161.8 MHz, C_6D_6): δ 169.0 (t), 150.2 (t), 147.7 (t), 147.2 (broad t), 63.7 (d), 48.3 (d), 45.0

(d), 29.6 (d), 29.2 (d). Purple crystals of **5** suitable for X-ray diffraction were grown by slow diffusion of Et_2O into a THF solution of the reaction mixture at room temperature.

Synthesis of 7. $Mo(CO)_3(C_7H_8)$ (0.172 g, 0.632 mmol) was dissolved in THF (12mL) and added to ligand ($PP^{I}P$) (0.465 g, 0.631 mmol). This dark red/orange solution was stirred for 16 hours at room temperature, then solvent was removed *in vacuo.* This film was rinsed with hexanes (6 mL), then lyophilized in benzene and dried *in vacuo* to yield a mixture of **6** and **7**, though **7** is the major product. Redissolving this mixture in THF (10 mL) and heating at 55°C for three days resulted in near-complete conversion to **7**. $^{31}P\{^{1}H\}$ NMR (161.8 MHz, C_6D_6): δ 327.9 (t, P^{NHP}, $^{2}J_{P\text{-}P}$ = 19.9 Hz, 1P), 17.6 (d, PPh_2, $^{2}J_{P\text{-}P}$ = 19.9 Hz, 2P).

Synthesis of unknown product 8. $B(C_6F_5)_3$ (0.009 g, 0.02 mmol) was dissolved in THF (6 mL) and added to **4** (0.014 g, 0.017 mmol). This orange solution was stirred for 2 days at room temperature, then solvent was removed *in vacuo* from the resulting solution. A 1:1 mixture of starting material **4** and new product **8** was observed. Addition of a 2nd equivalent of $B(C_6F_5)_3$ (0.008 g, 0.02 mmol) under the same conditions resulted in complete conversion to **8**. $^{31}P\{^{1}H\}$ NMR (161.8 MHz, C_6D_6): δ 150.4 (t, P^{NHP}, $^{2}J_{P\text{-}P}$ = 45.0 Hz, 1P), 49.3 (d, PPh_2, $^{2}J_{P\text{-}P}$ = 45.0 Hz, 2P).

Synthesis of 9-K. KHMDS (40.0 µL, 0.025 mmol) was dissolved in THF (8 mL) and added to **4** (0.020 g, 0.025 mmol). This solution immediately turned bright red and was stirred for 5 minutes at room temperature, then solvent was removed *in vacuo.* ^{31}P NMR (161.8 MHz, THF): δ 349 (t), 57 (d).

Synthesis of 10. $MoCl_3(THF)_3$ (0.128 g, 0.307 mmol) was dissolved in THF (12mL) and added to ligand ($PP^{Cl}P$) (0.199 g, 0.308 mmol). This dark red/orange solution was stirred for 16 hours at room temperature, then solvent was removed *in vacuo.* The resulting film was rinsed with benzene (6 mL) and solvent was again removed *in vacuo*. Small crystals were grown by slow diffusion of Et_2O into a THF solution of 10 at -35°C. However, none were rectangular enough to be suitable for X-ray diffraction.

Electrochemistry. Cyclic voltammetry measurements were carried out in a glovebox under a dinitrogen atmosphere in a one-compartment cell using a CH Instruments 620E electrochemical analyzer. A glassy carbon electrode, platinum wire, and $Ag/AgNO_3$ non-aqueous electrode were used as the working, auxiliary, and reference electrodes, respectively. THF solutions of supporting electrolyte (0.3 M $[^nBu_4N][PF_6]$) and analyte were also prepared in the glovebox. All potentials are reported versus the Fc/Fc^+ couple by comparison to an internal ferrocene reference that was added after data collection.

Computational Details. All calculations were performed using Gaussian16 for the Linux operating system[122] using computational resources through the Ohio Supercomputer Center.[123] DFT calculations were carried out using M06 functional.[119] Analytical frequency calculations were used to confirm that no imaginary frequencies were present. Single point NBO calculations for **2** were performed using NBO 3.1[124] as implemented in Gaussian16.

X-Ray Crystallography. Crystals of complexes **1**, **2**, **4**, and **5** were coated with paratone oil and mounted on a MiTeGen loop. All operations were performed on either a Bruker-Nonius Kappa Apex2 diffractometer or a Bruker D8 Venture PHOTON II CPAD system using graphite-monochromated Mo Kα radiation. All diffractometer manipulations, including data collection, integration, scaling, and absorption corrections were carried out using the Bruker Apex2[125] or Apex3[126] software.

References

(1) Arduengo, A. J.; Harlow, R. L.; Kline, M. A Stable Crystalline Carbene. *Journal of the American Chemical Society* **1991**, *113* (1), 361–363. https://doi.org/10.1021/ja00001a054.

(2) Crudden, C. M.; Allen, D. P. Stability and Reactivity of N-Heterocyclic Carbene Complexes. *Coordination Chemistry Reviews* **2004**, *248* (21–24), 2247–2273. https://doi.org/10.1016/j.ccr.2004.05.013.

(3) Budagumpi, S.; Keri, R. S.; Achar, G.; Brinda, K. N. Coinage Metal Complexes of Chiral N-Heterocyclic Carbene Ligands: Syntheses and Applications in Asymmetric Catalysis. *Advanced Synthesis and Catalysis* **2020**, *362* (5), 970–997. https://doi.org/10.1002/adsc.201900859.

(4) Pandey, M. K.; Choudhury, J. Ester Hydrogenation with Bifunctional Metal–NHC Catalysts: Recent Advances. *ACS Omega* **2020**. https://doi.org/10.1021/acsomega.0c04819.

(5) Peris, E.; Crabtree, R. H. Recent Homogeneous Catalytic Applications of Chelate and Pincer N-Heterocyclic Carbenes. *Coordination Chemistry Reviews* **2004**, *248* (21–24), 2239–2246. https://doi.org/10.1016/j.ccr.2004.04.014.

(6) Hopkinson, M. N.; Richter, C.; Schedler, M.; Glorius, F. An Overview of N-Heterocyclic Carbenes. *Nature* **2014**, *510* (7506), 485–496. https://doi.org/10.1038/nature13384.

(7) Herrmann, W. A. N-Heterocyclic Carbenes: A New Concept in Organometallic Catalysis. *Angewandte Chemie - International Edition* **2002**, *41* (8), 1290–1309. https://doi.org/10.1002/1521-3773(20020415)41:8<1290::AID-ANIE1290>3.0.CO;2-Y.

(8) Lin, J. C. Y.; Huang, R. T. W.; Lee, C. S.; Bhattacharyya, A.; Hwang, W. S.; Lin, I. J. B. Coinage Metal-N-Heterocyclic Carbene Complexes. *Chemical Reviews* **2009**, *109* (8), 3561–3598. https://doi.org/10.1021/cr8005153.

(9) Díez-González, S.; Marion, N.; Nolan, S. P. N-Heterocyclic Carbenes in Late Transition Metal Catalysis. *Chemical Reviews* **2009**, *109* (8), 3612–3676. https://doi.org/10.1021/cr900074m.

(10) Zhao, Q.; Meng, G.; Nolan, S. P.; Szostak, M. N-Heterocyclic Carbene Complexes in C-H Activation Reactions. *Chemical Reviews* **2020**, *120* (4), 1981–2048. https://doi.org/10.1021/acs.chemrev.9b00634.

(11) Liang, Q.; Song, D. Iron N-Heterocyclic Carbene Complexes in Homogeneous Catalysis. *Chemical Society Reviews* **2020**, *49* (4), 1209–1232. https://doi.org/10.1039/c9cs00508k.

(12) Hoveyda, A. H.; Zhou, Y.; Shi, Y.; Brown, M. K.; Wu, H.; Torker, S. Sulfonate N-Heterocyclic Carbene–Copper Complexes: Uniquely Effective Catalysts for Enantioselective Synthesis of C−C, C−B, C−H, and C−Si Bonds. *Angewandte Chemie - International Edition* **2020**, *59* (48), 21304–21359. https://doi.org/10.1002/anie.202003755.

(13) Rosenberg, L. Metal Complexes of Planar PR 2 Ligands: Examining the Carbene Analogy. *Coordination Chemistry Reviews* **2012**, *256* (5–8), 606–626. https://doi.org/10.1016/j.ccr.2011.12.014.

(14) Choudhury, J. N-Heterocyclic Nitrenium Ligands: A Missing Link Explored. *Angewandte Chemie - International Edition* **2011**, *50* (46), 10772–10774. https://doi.org/10.1002/anie.201104868.

(15) Tulchinsky, Y.; Iron, M. A.; Botoshansky, M.; Gandelman, M. Nitrenium Ions as Ligands for Transition Metals. *Nature Chemistry* **2011**, *3* (7), 525–531. https://doi.org/10.1038/nchem.1068.

(16) Tulchinsky, Y.; Kozuch, S.; Saha, P.; Mauda, A.; Nisnevich, G.; Botoshansky, M.; Shimon, L. J. W.; Gandelman, M. Coordination Chemistry of N-Heterocyclic Nitrenium-Based Ligands. *Chemistry - A European Journal* **2015**, *21* (19), 7099–7110. https://doi.org/10.1002/chem.201405526.

(17) Levy Vahav, H.; Pogoreltsev, A.; Tulchinsky, Y.; Fridman, N.; Börner, A.; Gandelman, M. Synthesis and Characteristics of Iridium Complexes Bearing N-Heterocyclic Nitrenium Cationic Ligands. *Organometallics* **2019**, *38* (12), 2494–2501. https://doi.org/10.1021/acs.organomet.9b00220.

(18) Heims, F.; Pfaff, F. F.; Abram, S. L.; Farquhar, E. R.; Bruschi, M.; Greco, C.; Ray, K. Redox Non-Innocence of a N-Heterocyclic Nitrenium Cation Bound to a Nickel-Cyclam Core. *Journal of the American Chemical Society* **2014**, *136* (2), 582–585. https://doi.org/10.1021/ja4099559.

(19) Yadav, S.; Deka, R.; Raju, S.; Singh, H. B. Synthesis of N-Heterocyclic Nitrenium (NHN) Ions and Related Donor Systems: Coordination with D10-Metal Ions. *Inorganica Chimica Acta* **2019**, *488* (January), 269–277. https://doi.org/10.1016/j.ica.2019.01.024.

(20) Zhou, J.; Liu, L. L.; Cao, L. L.; Stephan, D. W. Nitrogen-Based Lewis Acids: Synthesis and Reactivity of a Cyclic (Alkyl)(Amino)Nitrenium Cation. *Angewandte Chemie - International Edition* **2018**, *57* (13), 3322–3326. https://doi.org/10.1002/anie.201713118.

(21) Pazio, A.; Woźniak, K.; Grela, K.; Trzaskowski, B. Nitrenium Ions and Trivalent Boron Ligands as Analogues of N-Heterocyclic Carbenes in Olefin Metathesis: A Computational Study. *Dalton Transactions* **2015**, *44* (46), 20021–20026. https://doi.org/10.1039/c5dt03446a.

(22) Baker, R. J.; Jones, C.; Mills, D. P.; Pierce, G. A.; Waugh, M. Investigations into the Preparation of Groups 13-15 N-Heterocyclic Carbene Analogues. *Inorganica Chimica Acta* **2008**, *361* (2), 427–435. https://doi.org/10.1016/j.ica.2006.12.014.

(23) Burck, S.; Daniels, J.; Gans-Eichler, T.; Gudat, D.; Nättinen, K.; Nieger, M. N-Heterocyclic Phosphenium, Arsenium, and Stibenium Ions as Ligands in Transition Metal Complexes: A Comparative Experimental and Computational Study. *Zeitschrift fur Anorganische und Allgemeine Chemie* **2005**, *631* (8), 1403–1412. https://doi.org/10.1002/zaac.200400538.

(24) Spinney, H. A.; Korobkov, I.; Richeson, D. S. Diamidonaphthalene-Supported Pnictogenium Cations: Synthesis of an N-Heterocyclic Stibenium Cation by a Novel Protonation Route. *Chemical Communications* **2007**, No. 16, 1647–1649. https://doi.org/10.1039/b617434e.

(25) Dimroth, K.; Hoffmann, P. Phosphacyanines, a New Class of Compounds Containing Trivalent Phosphorus. *Angewandte Chemie International Edition in English* **1964**, *3* (5), 384–384. https://doi.org/10.1002/anie.196403841.

(26) Fleming, S.; Lupton, M. K.; Jekqt, A. K.; Fleming, S.; Lupton, M. K.; Jekqt, A. K. The Synthesis of a Cyclic Fluorodialkylaminophosphine and Its Coordination with Boron Acids. The Formation of a Unique Dialkylaminophosphine Cation. *Inorganic Chemistry* **1972**, *11* (10), 2534–2540. https://doi.org/10.1021/ic50116a050.

(27) Dixon, K. R. Phosphorus to Bismuth. *Multinuclear NMR* **1987**, 369–402. https://doi.org/10.1007/978-1-4613-1783-8_13.

(28) Day, G. S.; Pan, B.; Kellenberger, D. L.; Foxman, B. M.; Thomas, C. M. Guilty as Charged: Non-Innocent Behavior by a Pincer Ligand Featuring a Central Cationic Phosphenium Donor. *Chemical Communications* **2011**, *47* (12), 3634–3636. https://doi.org/10.1039/c0cc05739h.

(29) Spinney, H. A.; Yap, G. P. A.; Korobkov, I.; DiLabio, G.; Richeson, D. S. Construction of a Stable N-Heterocyclic Phosphenium Cation with an Electron-Rich Framework and Its Complexation to Rhodium. *Organometallics* **2006**, *25* (15), 3541–3543. https://doi.org/10.1021/om060466b.

(30) Dube, J. W.; Farrar, G. J.; Norton, E. L.; Szekely, K. L. S.; Cooper, B. F. T.; Macdonald, C. L. B. A Convenient Method for the Preparation of N-Heterocyclic Bromophosphines: Excellent Precursors to the Corresponding n-Heterocyclic Phosphenium Salts. *Organometallics* **2009**, *28* (15), 4377–4384. https://doi.org/10.1021/om900420g.

(31) Lyaskovskyy, V.; de Bruin, B. Redox Non-Innocent Ligands: Versatile New Tools to Control Catalytic Reactions. *ACS Catalysis* **2012**, *2* (2), 270–279. https://doi.org/10.1021/cs200660v.

(32) Habraken, E. R. M.; Jupp, A. R.; Brands, M. B.; Nieger, M.; Ehlers, A. W.; Slootweg, J. C. Parallels between Metal-Ligand Cooperativity and Frustrated Lewis Pairs. *European Journal of Inorganic Chemistry* **2019**, *2019* (19), 2436–2442. https://doi.org/10.1002/ejic.201900169.

(33) Khusnutdinova, J. R.; Milstein, D. Metal – Ligand Cooperation Angewandte. **2015**, 12236–12273. https://doi.org/10.1002/anie.201503873.

(34) Bielinski, E. A.; Lagaditis, P. O.; Zhang, Y.; Mercado, B. Q.; Würtele, C.; Bernskoetter, W. H.; Hazari, N.; Schneider, S. Lewis Acid-Assisted Formic Acid Dehydrogenation Using a Pincer-Supported Iron Catalyst. *Journal of the American Chemical Society* **2014**, *136* (29), 10234–10237. https://doi.org/10.1021/ja505241x.

(35) Chakraborty, S.; Lagaditis, P. O.; Förster, M.; Bielinski, E. A.; Hazari, N.; Holthausen, M. C.; Jones, W. D.; Schneider, S. Well-Defined Iron Catalysts for the Acceptorless Reversible Dehydrogenation-Hydrogenation of Alcohols and Ketones. *ACS Catalysis* **2014**, *4* (11), 3994–4003. https://doi.org/10.1021/cs5009656.

(36) Cronin, S. P.; Strain, J. M.; Mashuta, M. S.; Spurgeon, J. M.; Buchanan, R. M.; Grapperhaus, C. A. Exploiting Metal-Ligand Cooperativity to Sequester, Activate, and Reduce Atmospheric Carbon Dioxide with a Neutral Zinc Complex. *Inorganic Chemistry* **2020**, *59* (7), 4835–4841. https://doi.org/10.1021/acs.inorgchem.0c00121.

(37) Margulieux, G. W.; Bezdek, M. J.; Turner, Z. R.; Chirik, P. J. Ammonia Activation, H2 Evolution and Nitride Formation from a Molybdenum Complex with a Chemically and Redox Noninnocent Ligand. *Journal of the American Chemical Society* **2017**, *139* (17), 6110–6113. https://doi.org/10.1021/jacs.7b03070.

(38) Kounalis, E.; Lutz, M.; Broere, D. L. J. Cooperative H2 Activation on Dicopper(I) Facilitated by Reversible Dearomatization of an "Expanded PNNP Pincer" Ligand. *Chemistry - A European Journal* **2019**, *25* (58), 13280–13284. https://doi.org/10.1002/chem.201903724.

(39) Wong, J. L.; Higgins, R. F.; Bhowmick, I.; Cao, D. X.; Szigethy, G.; Ziller, J. W.; Shores, M. P.; Heyduk, A. F. Bimetallic Iron-Iron and Iron-Zinc Complexes of the Redox-Active ONO Pincer Ligand. *Chemical Science* **2016**, *7* (2), 1594–1599. https://doi.org/10.1039/c5sc03006d.

(40) Rosenkoetter, K. E.; Wojnar, M. K.; Charette, B. J.; Ziller, J. W.; Heyduk, A. F. Hydrogen-Atom Noninnocence of a Tridentate [SNS] Pincer Ligand. *Inorganic Chemistry* **2018**, *57* (16), 9728–9737. https://doi.org/10.1021/acs.inorgchem.8b00618.

(41) Jiang, Y.; Berke, H. Nitrosyl Complexes in Homogeneous Catalysis. In *Nitrosyl Complexes in Inorganic Chemistry, Biochemistry and Medicine I*; Mingos, D. M. P., Ed.; Springer Berlin Heidelberg: Berlin, Heidelberg, 2014; pp 167–228. https://doi.org/10.1007/430_2013_97.

(42) Enemark, J. H.; Feltham, R. D. Principles of Structure, Bonding, and Reactivity for Metal Nitrosyl Complexes. *Coordination Chemistry Reviews* **1974**, *13* (4), 339–406. https://doi.org/10.1016/S0010-8545(00)80259-3.

(43) Bower, J. K.; Sokolov, A. Y.; Zhang, S. Four-Coordinate Copper Halonitrosyl {CuNO}10 Complexes. *Angewandte Chemie - International Edition* **2019**, *58* (30), 10225–10229. https://doi.org/10.1002/anie.201904732.

(44) Parkin, G. A Simple Description of the Bonding in Transition-Metal Borane Complexes. *Organometallics* **2006**, *25* (20), 4744–4747. https://doi.org/10.1021/om060580u.

(45) Aullón, G.; Alvarez, S. Axial Bonding Capabilities of Square Planar D8-ML4 Complexes. Theoretical Study and Structural Correlations. *Inorganic Chemistry* **1996**, *35* (11), 3137–3144. https://doi.org/10.1021/ic951643w.

(46) Landry, V. K.; Melnick, J. G.; Buccella, D.; Pang, K.; Ulichny, J. C.; Parkin, G. Synthesis and Structural Characterization of [K3-B,S,S- B(MimR)3]Ir(CO)(PPh3)H (R = But, Ph) and [K4-B(MimBut)3]M(PPh3)Cl (M = Rh, Ir): Analysis of the Bonding in Metal Borane Compounds. *Inorganic Chemistry* **2006**, *45* (6), 2588–2597. https://doi.org/10.1021/ic051975t.

(47) Hill, A. F. An Unambiguous Electron-Counting Notation for Metallaboratranes. *Organometallics* **2006**, *25* (20), 4741–4743. https://doi.org/10.1021/om0602512.

(48) Cook, K. S.; Piers, W. E.; Woo, T. K.; McDonald, R. Reactions of Bis(Pentafluorophenyl)Borane with Cp2Ta(=CH2)CH3: Generation and Trapping of Tantalocene Borataalkene Complexes. *Organometallics* **2001**, *20* (18), 3927–3937. https://doi.org/10.1021/om010373o.

(49) Westcott, S. A.; Marder, T. B.; Baker, R. T.; Harlow, R. L.; Calabrese, J. C.; Lam, K. C.; Lin, Z. Reactions of Hydroborating Reagents with Phosphinorhodium Hydride Complexes: Molecular Structures of a Rh2B3 Metallaborane Cluster, an L2Rh(H2-H2BR2) Complex and a Mixed Valence Rh Dimer Containing a Semi-Bridging Bcat (Cat=1,2-O2C6H4) Group. *Polyhedron* **2004**, *23* (17 SPEC.ISS.), 2665–2677. https://doi.org/10.1016/j.poly.2004.05.012.

(50) Bontemps, S.; Gornitzka, H.; Bouhadir, G.; Miqueu, K.; Bourissou, D. Rhodium(I) Complexes of a PBP Ambiphilic Ligand: Evidence for a Metal→borane Interaction. *Angewandte Chemie - International Edition* **2006**, *45* (10), 1611–1614. https://doi.org/10.1002/anie.200503649.

(51) Wolczanski, P. T. Flipping the Oxidation State Formalism: Charge Distribution in Organometallic Complexes As Reported by Carbon Monoxide. *Organometallics* **2017**, *36* (3), 622–631. https://doi.org/10.1021/acs.organomet.6b00820.

(52) Birchall, N.; Feil, C. M.; Gediga, M.; Nieger, M.; Gudat, D. Reversible Cooperative Dihydrogen Binding and Transfer with a Bis-Phosphenium Complex of Chromium. *Chemical Science* **2020**, *11* (35), 9571–9576. https://doi.org/10.1039/d0sc03773g.

(53) Feil, C. M.; Hettich, T. D.; Beyer, K.; Sondermann, C.; Schlindwein, S. H.; Nieger, M.; Gudat, D. Comparing the Ligand Behavior of N-Heterocyclic Phosphenium and Nitrosyl Units in Iron and Chromium Complexes. *Inorganic Chemistry* **2019**, *58* (9), 6517–6528. https://doi.org/10.1021/acs.inorgchem.9b00737.

(54) Gediga, M.; Feil, C. M.; Schlindwein, S. H.; Bender, J.; Nieger, M.; Gudat, D. N-Heterocyclic Phosphenium Complex of Manganese: Synthesis and Catalytic Activity in Ammonia Borane Dehydrogenation. *Chemistry - A European Journal* **2017**, *23* (48), 11560–11569. https://doi.org/10.1002/chem.201701442.

(55) Papendick, M.; Feil, C. M.; Nieger, M.; Gudat, D. Steric Control in Reactions of N-Heterocyclic Phosphorus Electrophiles with Pentacarbonyl Manganate(–I). *Zeitschrift fur Anorganische und Allgemeine Chemie* **2018**, *644* (17), 1006–1010. https://doi.org/10.1002/zaac.201800178.

(56) Stadelmann, B.; Bender, J.; Förster, D.; Frey, W.; Nieger, M.; Gudat, D. An Anionic Phosphenium Complex as an Ambident Nucleophile. *Dalton Transactions* **2015**, *44* (13), 6023–6031. https://doi.org/10.1039/c5dt00008d.

(57) Pan, B.; Bezpalko, M. W.; Foxman, B. M.; Thomas, C. M. Coordination of an N-Heterocyclic Phosphenium Containing Pincer Ligand to a Co(CO) 2 Fragment Allows Oxidation to Form an Unusual N-Heterocyclic Phosphinito Species. *Organometallics* **2011**, *30* (21), 5560–5563. https://doi.org/10.1021/om200816p.

(58) Poitras, A. M.; Knight, S. E.; Bezpalko, M. W.; Foxman, B. M.; Thomas, C. M. Addition of H 2 Across a Cobalt-Phosphorus Bond . *Angewandte Chemie* **2018**, *130* (6), 1513–1516. https://doi.org/10.1002/ange.201710100.

(59) Hatzis, G. P.; Oliemuller, L. K.; Dickie, D. A.; Thomas, C. M. N-Heterocyclic Phosphido Complexes of Rhodium Supported by a Rigid Pincer Ligand. *European Journal of Inorganic Chemistry* **2020**, *2020* (30), 2873–2881. https://doi.org/10.1002/ejic.202000390.

(60) Pan, B.; Bezpalko, M. W.; Foxman, B. M.; Thomas, C. M. Heterolytic Addition of E-H Bonds across Pt-P Bonds in Pt N-Heterocyclic Phosphenium/Phosphido Complexes. *Dalton Transactions* **2012**, *41* (30), 9083–9090. https://doi.org/10.1039/c2dt30455d.

(61) Pan, B.; Xu, Z.; Bezpalko, M. W.; Foxman, B. M.; Thomas, C. M. N-Heterocyclic Phosphenium Ligands as Sterically and Electronically-Tunable Isolobal Analogues of Nitrosyls. *Inorganic Chemistry* **2012**, *51* (7), 4170–4179. https://doi.org/10.1021/ic202581v.

(62) Poitras, A. M.; Bezpalko, M. W.; Moore, C. E.; Dickie, D. A.; Foxman, B. M.; Thomas, C. M. A Series of Dimeric Cobalt Complexes Bridged by N-Heterocyclic Phosphido Ligands. *Inorganic Chemistry* **2020**, *59* (7), 4729–4740. https://doi.org/10.1021/acs.inorgchem.9b03790.

(63) Pan, B.; Evers-Mcgregor, D. A.; Bezpalko, M. W.; Foxman, B. M.; Thomas, C. M. Multimetallic Complexes Featuring a Bridging N-Heterocyclic Phosphido/Phosphenium Ligand: Synthesis, Structure, and Theoretical Investigation. *Inorganic Chemistry* **2013**, *52* (16), 9583–9589. https://doi.org/10.1021/ic4012873.

(64) Evers-McGregor, D. A.; Bezpalko, M. W.; Foxman, B. M.; Thomas, C. M. N-Heterocyclic Phosphenium and Phosphido Nickel Complexes Supported by a Pincer Ligand Framework. *Dalton Transactions* **2016**, *45* (5), 1918–1929. https://doi.org/10.1039/c5dt03549j.

(65) Nickolaus, J.; Bender, J.; Nieger, M.; Gudat, D. Sterically Controlled Synthesis and Nucleophilic Substitution Reactions of Di- and Trimeric n-Heterocyclic Phosphenium Metal(0) Halides. *European Journal of Inorganic Chemistry* **2014**, *2* (19), 3030–3036. https://doi.org/10.1002/ejic.201402137.

(66) Nakazawa, H. The Chemistry of Transition Metal Complexes Containing a Phosphenium Ligand. *Journal of Organometallic Chemistry* **2000**, *611* (1–2), 349–363. https://doi.org/10.1016/S0022-328X(00)00499-X.

(67) Montemayor, R. G.; Sauer, D. T.; Fleming, S.; Bennett, D. W.; Thomas, M. G.; Parry, R. W. Iron Carbonyl Complexes Containing Positively Charged Phosphorus Ligands. *Journal of the American Chemical Society* **1978**, *100* (7), 2231–2233. https://doi.org/10.1021/ja00475a044.

(68) Light, R. W.; Paine, R. T. Interaction of the Dicoordinate Phosphorus Cation l,3-Dimethyl-l,3,2-Diazaphospholidide with Transition Metal Nucleophiles. *Journal of the American Chemical Society* **1978**, *100* (7), 2230–2231.

(69) Abrams, M. B.; Scott, B. L.; Baker, R. T. Sterically Tunable Phosphenium Cations: Synthesis and Characterization of Bis(Arylamino)Phosphenium Ions, Phosphinophosphenium Adducts, and the First Well-Defined Rhodium Phosphenium Complexes. *Organometallics* **2000**, *19*, 4944–4956.

(70) Caputo, C. A.; Jennings, M. C.; Tuononen, H. M.; Jones, N. D. Phospha-Fischer Carbenes : Synthesis , Structure , Bonding , and Reactions of Pd (0) - and Pt (0) - Phosphenium Complexes. *Organometallic* **2009**, *28* (4), 990–1000. https://doi.org/https://doi.org/10.1021/om800973v.

(71) Caputo, C. A.; Brazeau, A. L.; Hynes, Z.; Price, J. T.; Tuononen, H. M.; Jones, N. D. A Cation-Captured Palladium(0) Anion: Synthesis, Structure, and Bonding of [PdBr(PPh3)2]- Ligated by an N-Heterocyclic Phosphenium Cation. *Organometallics* **2009**, *28* (17), 5261–5265. https://doi.org/10.1021/om9006278.

(72) Weller, S.; Schlindwein, S. H.; Feil, C. M.; Kelemen, Z.; Buzsáki, D.; Nyulászi, L.; Isenberg, S.; Pietschnig, R.; Nieger, M.; Gudat, D. A Ferrocenophane-Based Diaminophosphenium Ion. *Organometallics* **2019**, *38* (24), 4717–4725. https://doi.org/10.1021/acs.organomet.9b00701.

(73) Bezpalko, M. W.; Foxman, B. M.; Thomas, C. M. Use of a Bidentate Ligand Featuring an N-Heterocyclic Phosphenium Cation (NHP+) to Systematically Explore the Bonding of NHP+ Ligands with Nickel. *Inorganic Chemistry* **2015**, *54* (17), 8717–8726. https://doi.org/10.1021/acs.inorgchem.5b01363.

(74) Bezpalko, M. W.; Poitras, A. M.; Foxman, B. M.; Thomas, C. M. Cobalt N-Heterocyclic Phosphenium Complexes Stabilized by a Chelating Framework: Synthesis and Redox Properties. *Inorganic Chemistry* **2017**, *56* (1), 503–510. https://doi.org/10.1021/acs.inorgchem.6b02374.

(75) Yamaguchi, Y.; Nakazawa, H.; Kishishita, M.; Miyoshi, K. Reactivity of Cationic Phosphenium Complexes of Molybdenum: Migration of OR, SR, and NR2 on a Tertiary Phosphorus Compound to a Phosphenium Ligand. *Organometallics* **1996**, *15* (21), 4383–4388. https://doi.org/10.1021/om9600304.

(76) Snow, S. S.; Jiang, D.-X.; Parry, R. W. Formation of a Nickel Carbonyl Cation Containing a Cyclophosphenium Ligand by Hydride Abstraction. *Inorganic Chemistry* **1987**, *26*, 1629–1631.

(77) Olaru, M.; Mischin, A.; Malaspina, L. A.; Mebs, S.; Beckmann, J. The Bis(Ferrocenyl)Phosphenium Ion Revisited. *Angewandte Chemie - International Edition* **2020**, *59* (4), 1581–1584. https://doi.org/10.1002/anie.201913081.

(78) Caputo, C. A.; Price, J. T.; Jennings, M. C.; McDonald, R.; Jones, N. D. N-Heterocyclic Phosphenium Cations: Syntheses and Cycloaddition Reactions. *Dalton Transactions* **2008**, No. 26, 3461–3469. https://doi.org/10.1039/b801684d.

(79) Burck, S.; Gudat, D.; Nieger, M.; Schalley, C. A.; Weilandt, T. Phosphazene vs.Diazaphospholene PN-Bond Cleavage in Spirocyclic Cyclodiphosphazenes. *Dalton Transactions* **2008**, No. 26, 3478–3485. https://doi.org/10.1039/b717219b.

(80) Gudat, D.; Haghverdi, A.; Nieger, M. Umpolung of P-H Bonds. *Angewandte Chemie - International Edition* **2000**, *39* (17), 3084–3086. https://doi.org/10.1002/1521-3773(20000901)39:17<3084::AID-ANIE3084>3.0.CO;2-R.

(81) Burck, S.; Gudat, D.; Nieger, M.; du Mont, W.-W. P-Hydrogen-Substituted 1,3,2-Diazaphospholenes: Molecular Hydrides. *Journal of the American Chemical Society* **2006**, No. 128, 3946–3955.

(82) Zhang, J.; Yang, J. D.; Cheng, J. P. Diazaphosphinanes as Hydride, Hydrogen Atom, Proton or Electron Donors under Transition-Metal-Free Conditions: Thermodynamics, Kinetics, and Synthetic Applications. *Chemical Science* **2020**, *11* (14), 3672–3679. https://doi.org/10.1039/c9sc05883d.

(83) Chong, C. C.; Hirao, H.; Kinjo, R. A Concerted Transfer Hydrogenolysis: 1,3,2-Diazaphospholene-Catalyzed Hydrogenation of Ni-34;N Bond with Ammonia-Borane. *Angewandte Chemie - International Edition* **2014**, *53* (13), 3342–3346. https://doi.org/10.1002/anie.201400099.

(84) Chong, C. C.; Hirao, H.; Kinjo, R. Metal-Free σ-Bond Metathesis in 1,3,2-Diazaphospholene-Catalyzed Hydroboration of Carbonyl Compounds. *Angewandte Chemie - International Edition* **2015**, *54* (1), 190–194. https://doi.org/10.1002/anie.201408760.

(85) Rao, B.; Chong, C. C.; Kinjo, R. Metal-Free Regio- and Chemoselective Hydroboration of Pyridines Catalyzed by 1,3,2-Diazaphosphenium Triflate. *Journal of the American Chemical Society* **2018**, *140* (2), 652–656. https://doi.org/10.1021/jacs.7b09754.

(86) Ould, D. M. C.; Tran, T. T. P.; Rawson, J. M.; Melen, R. L. Structure-Property-Reactivity Studies on Dithiaphospholes. *Dalton Transactions* **2019**, *48* (45), 16922–16935. https://doi.org/10.1039/c9dt03577j.

(87) Adams, M. R.; Tien, C. H.; McDonald, R.; Speed, A. W. H. Asymmetric Imine Hydroboration Catalyzed by Chiral Diazaphospholenes. *Angewandte Chemie - International Edition* **2017**, *56* (52), 16660–16663. https://doi.org/10.1002/anie.201709926.

(88) Lundrigan, T.; Tien, C. H.; Robertson, K. N.; Speed, A. W. H. Air and Water Stable Secondary Phosphine Oxides as Diazaphospholene Precatalysts. *Chemical Communications* **2020**, *56* (58), 8027–8030. https://doi.org/10.1039/d0cc01072c.

(89) Lundrigan, T.; Welsh, E. N.; Hynes, T.; Tien, C. H.; Adams, M. R.; Roy, K. R.; Robertson, K. N.; Speed, A. W. H. Enantioselective Imine Reduction Catalyzed by Phosphenium Ions. *Journal of the American Chemical Society* **2019**, *141* (36), 14083–14088. https://doi.org/10.1021/jacs.9b07293.

(90) Miaskiewicz, S.; Reed, J. H.; Donets, P. A.; Oliveira, C. C.; Cramer, N. Chiral 1,3,2-Diazaphospholenes as Catalytic Molecular Hydrides for Enantioselective Conjugate Reductions. *Angewandte Chemie - International Edition* **2018**, *57* (15), 4039–4042. https://doi.org/10.1002/anie.201801300.

(91) Poitras, A. M.; Bezpalko, M. W.; Foxman, B. M.; Thomas, C. M. Cooperative Activation of O-H and S-H Bonds across the Co-P Bond of an N-Heterocyclic Phosphido Complex. *Dalton Transactions* **2019**, *48* (9), 3074–3079. https://doi.org/10.1039/c8dt05052j.

(92) Leischner, T.; Spannenberg, A.; Junge, K.; Beller, M. Molecular Defined Molybdenum-Pincer Complexes and Their Application in Catalytic Hydrogenations. *Organometallics* **2018**, *37* (23), 4402–4408. https://doi.org/10.1021/acs.organomet.8b00410.

(93) Castro-Rodrigo, R.; Chakraborty, S.; Munjanja, L.; Brennessel, W. W.; Jones, W. D. Synthesis, Characterization, and Reactivities of Molybdenum and Tungsten PONOP Pincer Complexes. *Organometallics* **2016**, *35* (18), 3124–3131. https://doi.org/10.1021/acs.organomet.6b00461.

(94) Benito-Garagorri, D.; Becker, E.; Wiedermann, J.; Lackner, W.; Pollak, M.; Mereiter, K.; Kisala, J.; Kirchner, K. Achiral and Chiral Transition Metal Complexes with Modularly Designed Tridentate PNP Pincer-Type Ligands Based on N-Heterocyclic Diamines. *Organometallics* **2006**, *25* (8), 1900–1913. https://doi.org/10.1021/om0600644.

(95) Öztopcu, Ö.; Holzhacker, C.; Puchberger, M.; Weil, M.; Mereiter, K.; Veiros, L. F.; Kirchner, K. Synthesis and Characterization of Hydrido Carbonyl Molybdenum and Tungsten PNP Pincer Complexes. *Organometallics* **2013**, *32* (10), 3042–3052. https://doi.org/10.1021/om400254k.

(96) Leischner, T.; Spannenberg, A.; Junge, K.; Beller, M. Synthesis of Molybdenum Pincer Complexes and Their Application in the Catalytic Hydrogenation of Nitriles. *ChemCatChem* **2020**, *12* (18), 4543–4549. https://doi.org/10.1002/cctc.202000736.

(97) Apps, S. L.; Alflatt, R. E.; Leforestier, B.; Storey, C. M.; Chaplin, A. B. Divergent Stereoisomers of Molybdenum Carbonyl Complexes of NHC-Based Pincer Ligands. *Polyhedron* **2018**, *143*, 57–61. https://doi.org/10.1016/j.poly.2017.08.001.

(98) Eder, W.; Stöger, B.; Kirchner, K. Synthesis and Characterization of Xylene-Based Group-Six Metal PCP Pincer Complexes. *Monatshefte fur Chemie* **2019**, *150* (7), 1235–1240. https://doi.org/10.1007/s00706-019-02422-6.

(99) Himmelbauer, D.; Mastalir, M.; Stöger, B.; Veiros, L. F.; Kirchner, K. Synthesis and Reactivity of Group Six Metal PCP Pincer Complexes: Reversible CO Addition Across the Metal-Caryl Bond. *Organometallics* **2018**, *37* (20), 3631–3638. https://doi.org/10.1021/acs.organomet.8b00447.

(100) de Aguiar, S. R. M. M.; Schröder-Holzhacker, C.; Pecak, J.; Stöger, B.; Kirchner, K. Synthesis and Characterization of TADDOL-Based Chiral Group Six PNP Pincer Tricarbonyl Complexes. *Monatshefte fur Chemie* **2019**, *150* (1), 103–109. https://doi.org/10.1007/s00706-018-2281-0.

(101) Zhang, Y.; Williard, P. G.; Bernskoetter, W. H. Synthesis and Characterization of Pincer-Molybdenum Precatalysts for CO2 Hydrogenation. *Organometallics* **2016**, *35* (6), 860–865. https://doi.org/10.1021/acs.organomet.5b00955.

(102) Itabashi, T.; Arashiba, K.; Tanaka, H.; Konomi, A.; Eizawa, A.; Nakajima, K.; Yoshizawa, K.; Nishibayashi, Y. Synthesis and Catalytic Reactivity of Bis(Molybdenum-Trihalide) Complexes Bridged by Ferrocene Skeleton toward Catalytic Nitrogen Fixation. *Organometallics* **2019**, *38* (14), 2863–2872. https://doi.org/10.1021/acs.organomet.9b00263.

(103) Itabashi, T.; Mori, I.; Arashiba, K.; Eizawa, A.; Nakajima, K.; Nishibayashi, Y. Effect of Substituents on Molybdenum Triiodide Complexes Bearing PNP-Type Pincer Ligands toward Catalytic Nitrogen Fixation. *Dalton Transactions* **2019**, *48* (10), 3182–3186. https://doi.org/10.1039/c8dt04975k.

(104) Arashiba, K.; Eizawa, A.; Tanaka, H.; Nakajima, K.; Yoshizawa, K.; Nishibayashi, Y. Catalytic Nitrogen Fixation via Direct Cleavage of Nitrogen-Nitrogen Triple Bond of Molecular Dinitrogen

under Ambient Reaction Conditions. *Bulletin of the Chemical Society of Japan* **2017**, *90* (10), 1111–1118. https://doi.org/10.1246/bcsj.20170197.

(105) Stucke, N.; Krahmer, J.; Näther, C.; Tuczek, F. Molybdenum Complexes Supported by PN3P Pincer Ligands: Synthesis, Characterization, and Application to Synthetic Nitrogen Fixation. *European Journal of Inorganic Chemistry* **2018**, *2018* (47), 5108–5116. https://doi.org/10.1002/ejic.201801194.

(106) Oelkers, B.; Venker, A.; Sundermeyer, J. Molybdenum 1,4-Diazabuta-1,3-Diene Tricarbonyl Solvento Complexes Revisited: From Solvatochromism to Attractive Ligand-Ligand Interaction. *Inorganic Chemistry* **2012**, *51* (8), 4636–4643. https://doi.org/10.1021/ic202517w.

(107) Ainscough, E. W.; Brodie, A. M.; Buckley, P. D.; Burrell, A. K.; Kennedy, S. M. F.; Waters, J. M. Synthesis, Structure and Kinetics of Group 6 Metal Carbonyl Complexes Containing a New ′P2N′ Mixed Donor Multidentate Ligandt. *Journal of the Chemical Society, Dalton Transactions* **2000**, No. 16, 2663–2671. https://doi.org/10.1039/b002427i.

(108) Goren Keskin, S.; Stanley, J. M.; Cowley, A. H. Synthesis, Characterization and Theoretical Investigations of Molybdenum Carbonyl Complexes with Phosphorus/Nitrogen/Phosphorus Ligand as Bidentate and Tridentate Modes. *Polyhedron* **2017**, *138*, 206–217. https://doi.org/10.1016/j.poly.2017.09.037.

(109) Keskin, S. G.; Mejia, M. L.; Cowley, A. H.; Holliday, B. J. Molybdenum Carbonyl Complexes with a Polymerizable Phosphorus/Nitrogen/Phosphorus Ligand and Corresponding Conducting Metallopolymers. *Macromolecular Chemistry and Physics* **2018**, *219* (22), 1–14. https://doi.org/10.1002/macp.201800262.

(110) Downing, S. P.; Hanton, M. J.; Slawin, A. M. Z.; Tooze, R. P. Bis(Alkylthioethyl)Amine Complexes of Molybdenum. *Organometallics* **2009**, *28* (8), 2417–2422. https://doi.org/10.1021/om9000346.

(111) Laube, J.; Thöne, C. The Novel Multidentate Ligands TBU2P(2-SePy) and TBUP(2-SePy)2; Py = Pyridyl. Synthesis, Reactivity and Crystal Structures of Mo-, Cu- and Ag-Complexes. *Phosphorus, Sulfur and Silicon and Related Elements* **2001**, *168–169*, 173–176. https://doi.org/10.1080/10426500108546618.

(112) Takuma, M.; Ohki, Y.; Tatsumi, K. Molybdenum Carbonyl Complexes with Citrate and Its Relevant Carboxylates. *Organometallics* **2005**, *24* (6), 1344–1347. https://doi.org/10.1021/om049072f.

(113) Lowry, D. J.; Helm, M. L. Synthesis of 1,4,7-Triphenyl-1,4,7-Triphosphacyclononane: The First Metal-Free Synthesis of a [9]-AneP3R3 Ring. *Inorganic Chemistry* **2010**, *49* (11), 4732–4734. https://doi.org/10.1021/ic100274m.

(114) Mayer, H. A.; Stößel, P.; Fawzi, R.; Steimann, M. Synthesis and X-Ray Molecular Structure of Cis, Cis-1,3,5-Tris(Diphenylphosphino)- 1,3,5-Tris(Methoxycarbonyl) Cyclohexane. *Journal of Organometallic Chemistry* **1995**, *492* (1), 50–52. https://doi.org/10.1016/0022-328X(94)05316-4.

(115) Garcfa, F.; Hopkins, A. D.; Kowenicki, R. A.; McPartlin, M.; Rogers, M. C.; Silvia, J. S.; Wright, D. S. Syntheses and Structure of Heterometallic Complexes Containing Tripodal Group 13 Ligands [RE(2-Py)3]- (E = Al, In). *Organometallics* **2006**, *25* (10), 2561–2568. https://doi.org/10.1021/om0600691.

(116) Joseph, C.; Kuppuswamy, S.; Lynch, V. M.; Rose, M. J. Fe5Mo Cluster with Iron-Carbide and Molybdenum-Carbide Bonding Motifs: Structure and Selective Alkyne Reductions. *Inorganic Chemistry* **2018**, *57* (1), 20–23. https://doi.org/10.1021/acs.inorgchem.7b02615.

(117) Mandal, S.; Qian, M.; Reber, A. C.; Saavedra, H. M.; Weiss, P. S.; Khanna, S. N.; Sen, A. 3- M = Cr, Mo, W: Bonding and Electronic Structure of Cluster Assemblies with Metal Carbonyls. *Journal of Physical Chemistry C* **2011**, *115* (48), 23704–23710. https://doi.org/10.1021/jp207268x.

(118) Luh, T. Y. Trimethylamine N-Oxide-a Versatile Reagent for Organometallic Chemistry. *Coordination Chemistry Reviews* **1984**, *60* (C), 255–276. https://doi.org/10.1016/0010-8545(84)85067-5.

(119) Fürstner, A.; Mathes, C.; Lehmann, C. W. Alkyne Metathesis: Development of a Novel Molybdenum-Based Catalyst System and Its Application to the Total Synthesis of Epothilone A and C. *Chemistry - A European Journal* **2001**, *7* (24), 5299–5317. https://doi.org/10.1002/1521-3765(20011217)7:24<5299::AID-CHEM5299>3.0.CO;2-X.

(120) Wickramasinghe, L. A.; Ogawa, T.; Schrock, R. R.; Müller, P. Reduction of Dinitrogen to Ammonia Catalyzed by Molybdenum Diamido Complexes. *Journal of the American Chemical Society* **2017**, *139* (27), 9132–9135. https://doi.org/10.1021/jacs.7b04800

(121) Oliemuller, L. K.; Moore, C. E.; Thomas, C. M. "Synthesis and Characterization of Novel Binding Modes in Pincer-Ligated N-Heterocyclic Phosphenium/Phosphido Nickel Complexes." *Manuscript in preparation.*

(122) Frisch, M. J.; Trucks, G. W.; Schlegel, H. B.; Scuseria, G. E.; Robb, M. A.; Cheeseman, J. R.; Scalmani, G.; Barone, V.; Petersson, G. A.; Nakatsuji, H.; Li, X.; Caricato, M.; Marenich, A. V.; Bloino, J.; Janesko, B. G.; Gomperts, R.; Mennucci, B.; Hratchian, H. P.; Ortiz, J. V.; Izmaylov, A. F.; Sonnenberg, J. L.; Williams; Ding, F.; Lipparini, F.; Egidi, F.; Goings, J.; Peng, B.; Petrone, A.; Henderson, T.; Ranasinghe, D.; Zakrzewski, V. G.; Gao, J.; Rega, N.; Zheng, G.; Liang, W.; Hada, M.; Ehara, M.; Toyota, K.; Fukuda, R.; Hasegawa, J.; Ishida, M.; Nakajima, T.; Honda, Y.; Kitao, O.; Nakai, H.; Vreven, T.; Throssell, K.; Montgomery Jr., J. A.; Peralta, J. E.; Ogliaro, F.; Bearpark, M. J.; Heyd, J. J.; Brothers, E. N.; Kudin, K. N.; Staroverov, V. N.; Keith, T. A.; Kobayashi, R.; Normand, J.; Raghavachari, K.; Rendell, A. P.; Burant, J. C.; Iyengar, S. S.; Tomasi, J.; Cossi, M.; Millam, J. M.; Klene, M.; Adamo, C.; Cammi, R.; Ochterski, J. W.; Martin, R. L.; Morokuma, K.; Farkas, O.; Foresman, J. B.; Fox, D. J. Gaussian 16 Rev. C.01, Wallingford, CT, 2016.

(123) Ohio Supercomputer Center. Columbus, OH, 1987.

(124) Glendening, E. D.; Reed, A. E.; Carpenter, J. E.; Weinhold, F. NBO Version 3.1.

(125) Apex 2: Version 2 User Manual, M86-E01078. Bruker Analytical X-ray Systems: Madison, WI, 2006.

(126) Bruker Saint; SADABS; APEX3., Bruker AXS Inc.: Madison, Wisconsin, USA, 2012.